European Journal of Wood and Wood Products (2023) 81:633–654
https://doi.org/10.1007/s00107-022-01918-z

ORIGINAL ARTICLE

Capacity models for timber under compression perpendicular to grain with screw reinforcement

Angelo Aloisio[1,2] · Ebenezer Ussher[2] · Massimo Fragiacomo[1] · Roberto Tomasi[2]

Received: 14 August 2022 / Accepted: 20 December 2022 / Published online: 11 January 2023

Abstract
This paper compares the performance of probabilistic and deterministic capacity models for reinforced timber members under compression perpendicular to the grain. A database collecting approximately 60 test results has been compiled by reviewing research papers and master's and doctoral theses from the past twenty years. The capacity model proposed for the next generation of Eurocodes assesses the capacity as the minimum between the values associated with two failure modes, one at the contact plate and one at the screw tips. The main drawbacks of the model are the excessive elaborateness, given its limitation in accuracy and the fallacy in predicting the observed failure modes. In detail, the failure by the screw tips seldom occurs, although it was expected in more than half of the selected specimens. The authors attempted to simplify the capacity equation by proposing a generalized expression corresponding to the failure mode at the contact plate, corrected by a factor including the effects of load and screw arrangement and geometric details of the specimen. A deterministic mechanical model obtained by multiplying the timber strength by the contact area with a given coefficient performs better than the Eurocode model, which attempts to include the effect of load diffusion ($R^2 \approx 0.27$). A constant factor equal to 2 yields a suitable fitting ($R^2 \approx 0.76$). The best performance is achieved with a four-term polynomial, with adimensional addends, leading to an optimum fitting ($R^2 \approx 0.82$).

1 List of symbols and notations

- A_1 and A_2: CPG capacities associated with two failure mechanisms: the first by the contact area of the load and the second by the screw tips.
- A_{11} and A_{11}^*: Timber contribution to the capacity under CPG. A_{11} is calculated with Eq. 5 considering an effective spreading length ($l_{ef,1}$). A_{11}^*, calculated using Eq. 20, neglects any sort of load diffusion.
- A_{12}: Screw contribution to the capacity under CPG, calculated with Eq. 5.
- A_{ef}: Effective contact area. Due to the contribution of adjacent fibres, an increase of 30 mm of the contact length on each side of the contact area is recommended.
- a_1: Spacing between screw or rod reinforcement in the direction parallel to the grain.
- $a_{3,c}$: Distance between the screw closest to the member edge and the member end in the direction parallel to the grain.
- α: Angle between screw axis and grain direction of the wood member.
- B_1: CPG capacity of the un-reinforced timber specimen.
- b: Member width.
- b_c: Width of the contact area for the reinforced member under CPG.
- $c_h = (0.19 + 0.012d)\rho_k\left(\frac{90°+\alpha}{180}\right)$: Sub-grade coefficient for the screw for solid timber, glued laminated (GL) timber of softwood. c_h is in MPa if d is in mm, ρ_k in kg/m^3 and α in degrees.
- CPG: Compression perpendicular to the grain.

✉ Angelo Aloisio
angelo.aloisio1@univaq.it

Ebenezer Ussher
ebenezer.ussher@nmbu.no

Massimo Fragiacomo
massimo.fragiacomo@univaq.it

Roberto Tomasi
roberto.tomasi@nmbu.no

[1] Department of Civil, Construction-Architectural and Environmental Engineering, Università degli Studi dell'Aquila, 67100, L'Aquila, Italy

[2] Faculty of Science and Technology, Norwegian University of Life Sciences, Oslo, Norway

- CoV: Coefficient of Variation.
- $C(\mathbf{x}, \boldsymbol{\Theta})$: Following Gardoni et al. (2002), it is the capacity, where $\mathbf{x}$ are the measurable capacity variables, and $\boldsymbol{\Theta} = \{\theta, \sigma\}$ are unknown model parameters with modeling error σ.
- d: Outer thread diameter of the screw;
- d_1: Inner thread diameter of the screw obtained as $0.7d$;
- E_s: Young's modulus of steel equals to 210GPa.
- θ_{ij}: Generic coefficient of the explanatory variables used in the probabilistic capacity models.
- $f_{c,90,d}$: Design compression strength perpendicular to the grain direction.
- $F_{c,90,d}$: Design compression force perpendicular to the grain direction.
- $F_{c,90,k}$: Characteristic compressive strength of the reinforced member under CPG.
- $F^{j}_{c,90,m}$: Mean compressive strength of the reinforced member under CPG, where the index j indicates the model number used for its estimation. The paper investigates eight capacity models, so $j \in [1-8]$.
- $f_{c,90,k}$: Characteristic compressive strength of the reinforced member under CPG.
- $F_{w,k}$: Characteristic withdrawal capacity of the screw.
- $f_{w,k}$: Characteristic withdrawal strength of the screw. The definition of $f_{w,k}$, reported in Eq. 8, follows Eq.6 in Tab.11.2 of the Eurocode 5 draft (2022).
- $F_{c,k}$: Characteristic axial capacity of the screw.
- F_{exp}: Experimental capacity under CPG.
- $f_{y,k}$: Characteristic yielding strength of the steel.
- γ_1 and γ_2: Correction factors (Eqs. 25, 26) used in the two probabilistic capacity models.
- γ_3: Constant coefficient, found equal to 1.2, used in the proposed deterministic capacity model.
- h_{ef}: Effective height. For members on continuous support loaded by concentrated forces perpendicular to the grain, the load arrangement factor should be calculated with an effective spreading length of the compressive stresses. The following equations should be used for continuous and discrete supports respectively: $h_{ef} = \min\{h;280\text{mm}\}$, $h_{ef} = \min\{0.4 \cdot h;140\text{mm}\}$.
- $I_s = \pi \cdot \frac{d_1^4}{64}$: Moment of inertia of the screws cross-sections.
- $k_{c,90}$: load distribution factor and equal to $\sqrt{l_{ef}/l_c}$ for unreinforced members.
- $k = 0.5\left[1 + 0.49\left(\bar{\lambda}_k - 0.2\right) + \bar{\lambda}_k^2\right]$: Buckling coefficient for buckling.
- k_p for un-reinforced compression perpendicular to grain: according to prEN1995 (2021), it accounts for the material behaviour and the degree of deformation perpendicular to the grain. The factor accounts for the increased stiffness when the deformation increases (Leijten et al. 2012), see Table 1.

Table 1 Values for k_p from prEN 1995 for un-reinforced case, valid for solid timber, glulam, and CLT

Cases	Case A	Case B	Case C
Deformation	2.50%	10%	20%
k_p factor	1.4	2.1	2.7

Table 2 Reduction factors due to buckling, where α is the angle between screw axis and grain

f_{yk} [Mpa]	α=90	α=0
1000	0.6	0.5
800	0.65	0.55
500	0.75	0.65

- k_{pr} parameter adopted for screws reinforced compression perpendicular to the grain (this parameter was originally indicated as $k_{c,90}$ in EN 1995-1-1): according to prEN1995-1-1, it takes into account the material behaviour and the degree of deformation perpendicular to the grain. The value of k_{pr} according to Blass et al. (2004) and the existing version of (EN1995 2010) can be assumed as 1.75 for glulam members on discrete supports loaded by distributed loads and/or by concentrated loads at a clear distance from the support l_s larger or equal to $2h$, or 1.5 in case of glulam member on continuous support (sill configuration). For the other cases, the value of k_{pr} can be assumed equal to 1. The tested specimens correspond to the left scenario in Fig. 1.
- $k_w = \begin{cases} 1, & 30° \le \epsilon \le 90° \\ 1 - 0.01(30° - \epsilon), & 0° \le \epsilon < 30° \end{cases}$: Parameter for screws and rods with wood-screw thread, where ϵ is the angle between the fastener axis and the direction of the grain.
- $k_{mat} = \begin{cases} 1.0, & n_p = 1 \\ 1.06, & n_p \ge 2 \\ 1.10, & n_p \ge 3 \\ 1.13, & n_p \ge 5 \\ 1.15, & n_p \ge 7 \end{cases}$: Material parameter for the number of lamination, where n_p is the number of lamination.
- $k_\rho = \begin{cases} 1.10, & \text{for softwoods and } 15° \le \epsilon \le 90° \\ 1.25 - 0.05d, & \text{for softwoods and } 0° \le \epsilon < 15° \\ 1.6, & \text{for hardwoods and } 0° \le \epsilon \le 90° \end{cases}$: Parameter for screws and rods with wood-screw thread, where ϵ is the angle between the fastener axis and the direction of the grain.
- $\kappa_c = \begin{cases} 1, & \bar{\lambda}_k \le 0.2 \\ \frac{1}{k + \sqrt{k^2 - \bar{\lambda}_k^2}}, & \bar{\lambda}_k > 0.2 \end{cases}$: Reduction factors for screw buckling. Alternatively, the values in Table 2 can be used. For values non-included in Table 2 the linear interpolation should be carried out.

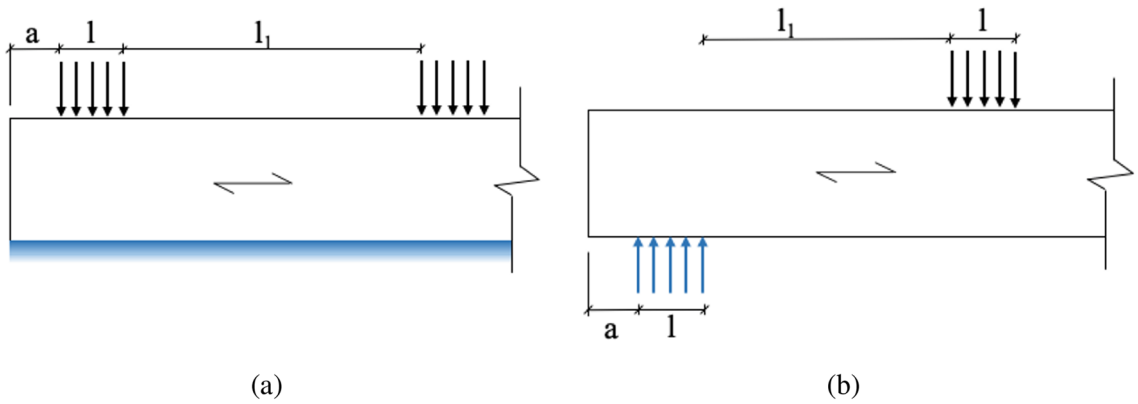

Fig. 1 CPG according to NS-EN1995-1-1, continuous support (**a**) and discrete support (**b**)

- $l_{ef,1}$: Effective contact length parallel to the grain in correspondence with the contact area for the reinforced member under CPG.
- $l_{ef,2}$: Effective distribution length parallel to the grain defined by the screw or rod types for the reinforced member under CPG.
- l_e: Clear spacing parallel to grain between the contact area and the member edge.
- l_r: Penetration part of the threaded part of the screw.
- l_s: Length support to concentrated load. The Karlsruhe model indicated the penetration part of the threaded part of the screw (l_r).
- l_{ef}: Effective spreading length of the compressive stresses estimated by assuming a 45° diffusion angle.
- l_c: Contact length of the applied force.
- l_w: Anchorage depth of the screw.
- $\bar{\lambda}_k = \frac{N_{pl,k}}{N_{ki,k}}$: Relative slenderness ratio of the screws.
- n: Number of fully threaded screws.
- n_0: Number of fully threaded screws or rods arranged in a row parallel to the grain.
- $N_{pl,k}$: Characteristic buckling strength of the screw.
- $N_{ki,k} = 2\sqrt{c_h E_s I_s}$: Characteristic ideal elastic buckling.
- ρ_k: Characteristic density of wood.
- $R_{S,k}$: In the Karlsruhe model it indicates the minimum between $F_{c,k}$ and $F_{w,k}$.
- $R_{ax,k}$: In the Karlsruhe model, it indicated the withdrawal strength of the screw, named $F_{w,k}$ in the current notation.
- $R_{c,k}$: In the Karlsruhe model, it indicated the buckling strength of the screw, named $F_{c,k}$ in the current notation.
- $\sigma_{c,90,d}$: design compression stress perpendicular to the grain direction.

2 Introduction

Timber is a highly anisotropic material: the direction of the grain influences its mechanical properties (Porteous and Kermani 2013). In the direction parallel to the grain, timber is strong and stiff. On the contrary, in the direction perpendicular to the grain, the strength and stiffness are relatively lower (Porteous and Kermani 2013; Augustin et al. 2006). The fibres in timber are tubular and elongated. Therefore, the compression perpendicular to grain (CPG) failure leads to a collapse of the cellular tubes, manifesting as failure along the tubular layers (Persson 2000; Swedish Wood Stockholm, Sweden 2016), see Fig. 2.

Beams, trusses, and supports are typical design situations where CPG can occur (Hassan et al. 2014). Failure due to CPG does not generally lead to collapse. The failure in CPG is potentially a concern in the serviceability limit state (SLS). Yet, in Eurocode 5, CPG is regarded as an ultimate limit state (ULS) problem to avoid load failure of structural systems (Forening, Norske Limtreprodusenters Norway 2015). The failure mode due to the CPG occurs on the contact area of the load; see Fig. 3: as the compressive load increases, the fibres buckle. This compression will transmit to neighbouring fibres as a chain reaction. Higher loads can be achieved with higher deformation levels and dispersion lengths (Forening, Norske Limtreprodusenters Norway 2015).

The strength under CPG can be improved by using suitable reinforcements. Past and recent research (Bejtka 2005; Dietsch et al. 2015; Dietsch and Brandner 2015; Harte et al. 2015; De Santis and Fragiacomo 2021) prove

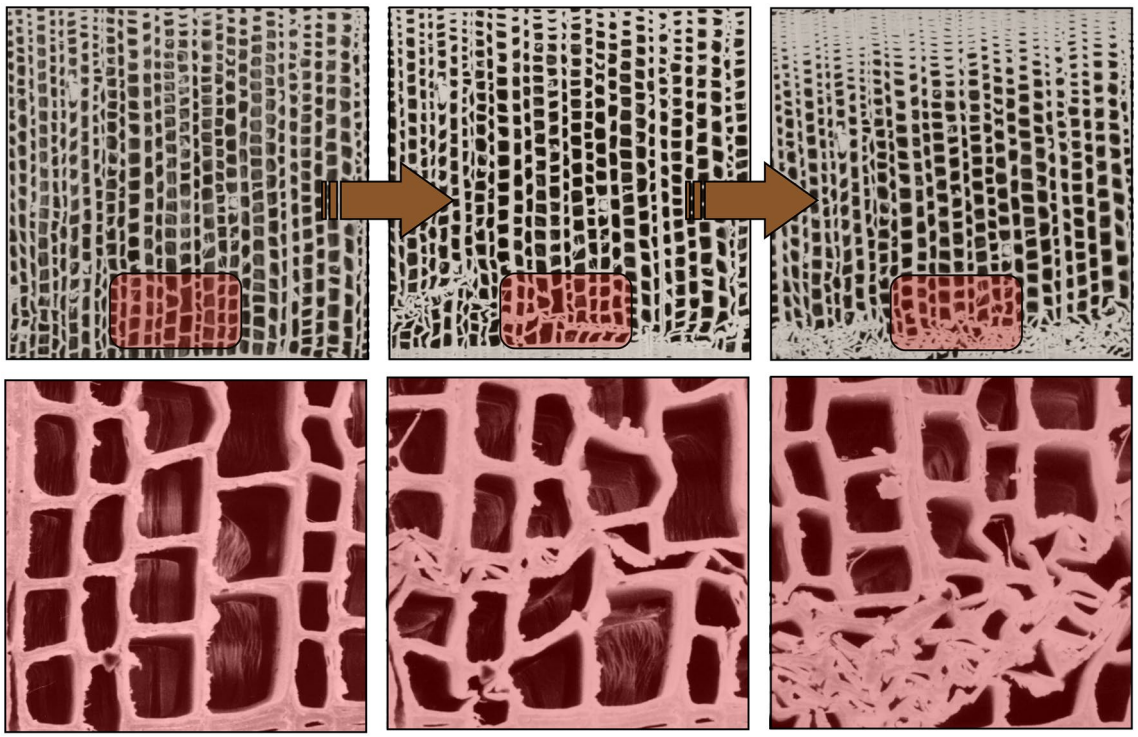

Fig. 2 Illustration of the effect of compression perpendicular to the grain (CPG) on timber microstructure. From left to right, the figure shows the undeformed configuration, the failure of a single layer, and the failure of multiple layers (Persson 2000).

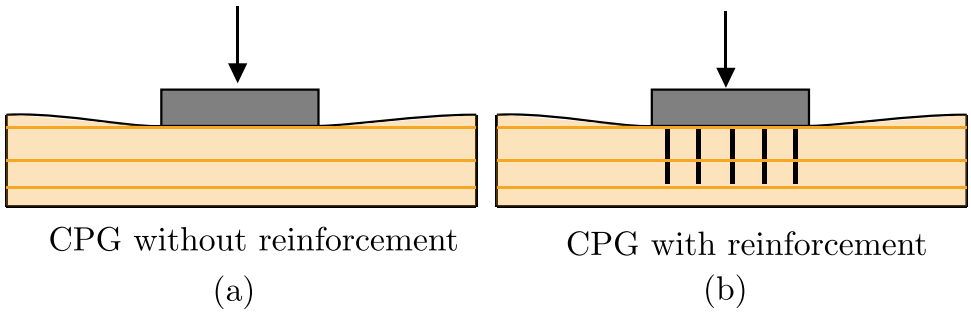

Fig. 3 Illustration of a timber specimen without (a) and with (b) screw reinforcement under CPG.

that self-tapping screws are the most effective reinforcement system for timber under CPG (Kreuzinger 1999, 2001, 2002). Screws can also be used to strengthen notches, holes in beams (Aicher and Höfflin 2002, 2003; Kolb 2008; Aicher et al. 2007; Aicher and Höfflin 2009; Aicher 2011), or against tension stress perpendicular to the grain in curved or pitched cambered beams (Eurocode 2010; Tomasi et al. 2010).

Other techniques have been identified in improving the CPG of timber members. Nonetheless, reinforcement, glued-in rods or steel screws are not prescribed in Code (2005). For practical applications, screws recommended for the reinforcement of timber perpendicular to the grain are regulated by European Technical Approvals (ETA 2019), which are supplier-specific (O'Ceallaigh and Harte 2019).

Apart from screws, dowels also proved to be effective reinforcement systems of timber under CPG. Madsen et al. (2000) successfully installed steel dowels perpendicular to grain through the full height of glulam beams. Ed and Hasselqvist (2011) performed similar tests using birch dowels to enhance the compressive strength of glulam beams. Still, using self-tapping screws is the most favoured method for timber reinforcement due to several advantages. They are easy to install and may be used in various applications: to prevent splitting perpendicular to the grain, enhance dowel embedment strength, or enhance strength perpendicular-to-grain (Bejtka and Blaß 2004). Screw reinforcements can be used for in-situ and off-site manufactured frames/panels (Kildashti et al. 2021; Alinoori et al. 2020). Bejtka (2005) was among the first to study the effect of reinforcement in

CPG. Pampanin (2013) used self-tapping screws to reinforce laminated veneer lumber (LVL) beams, while Dietsch et al. (2019) performed similar tests on glulam beams.

In the last decade, reinforcement under CPG is also becoming relevant for Cross Laminated Timber (CLT) elements (Mestek 2011). Serrano and Enquist (2010) tested 3-ply CLT elements and found the compressive strength dependent on the bearing area, load orientation to the surface grain, and loading positions. Bogensperger et al. (2011) compared data from glulam and CLT specimens and determined strength under CPG. Lately, Brandner (2018) published a state-of-the-art review on CLT loaded in compression perpendicular-to-plane, where a load-spreading model is proposed (van der Put 2012). Recently, Rothoblaas developed the SPIDER system to enhance the CPG strength of point-supported CLT floor systems using a steel element (Maurer and Maderebner 2021).

Steel is not the sole solution for reinforcing timber under CPG. However, there is growing mainstream research on using timber-based elements as reinforcement. In detail, some research papers propose using hardwood or densified wood dowels as reinforcement perpendicular to the grain (Conway et al. 2020, 2021; Moerman et al. 2021). This solution showed significant potential in improving the load-carrying capacity of timber perpendicular to the grain (Crocetti et al. 2012; Ed and Hasselqvist 2011), despite being outperformed by steel screw alternatives (Orlando et al. 2019).

The use of screw reinforcement for CPG is now an acknowledged solution. The draft of the next generation of Eurocodes, including a section on this topic, confirms this fact. Nonetheless, the knowledge of the actual effect of screws on the timber strength under CPG is still embryonal. The investigation of the CPG without reinforcement has a more extended chronology. Still, Leijten (2016) dashingly states that current CPG models are unreliable, and there is only one accurate model based on yield slip-line theory to be a candidate for future building design codes. He reviewed several past studies, partially itemized below, on CPG tests. They were all discarded due to misconceptions, inaccuracy or lack of adequate methodological rigour; see the studies by Kollmann et al. (2012); Graf (1921); Gehri (1997); Hübner (2013); Gaber (1940); Frey-Wyssling and Stüssi (1948); Rothmund (1944). In North America, Basta (2005) carried out CPG tests according to ASTM-D-143 (ASTM 1991), including the wood species, moisture, and annual ring orientation effects. The research by Basta (2005) was considered irrelevant since the definition of the CPG values obtained with this method was based on the proportional limit. In contrast, it is now based on a 1% deformation limit according to the standard EN 408 (EN408 2012). Hoffmeyer et al. (2000) report tests on 74 sawn timber specimens and 120 glued laminated specimens having a mean CPG strength of 2.9 N/mm^2. Hoffmeyer et al. (2000) found that CPG strength does not change significantly with the specimen dimensions.

The first studies on CPG without reinforcement were carried out by Suenson (1938a). The tests highlighted that the CPG capacity depends on the loading area and the length of the unloaded part (Leijten 2016). Multiple studies confirmed these aspects in the following years (Reichegger 2004). Leijten (2016) compared different design models for CPG without reinforcement and presented nine load cases, shown in Fig. 4. The load cases distinguish different design configurations, except for load case A, defined by EN 408. In this paper, the authors will adopt the designations in Fig. 4 to identify the different load cases.

If, according to Madsen et al. (1982), CPG did not receive sufficient attention from the scientific community, CPG with reinforcement received even less (Thelandersson and Mårtensson 1997; Kevarinmäki 1992). No paper attempts to review and compare existing capacity models for CPG with reinforcement. Additionally, the deficiency of organic research in this area is further fed by exiguous experimental data. This paper attempts to fill the mentioned gap in knowledge by investigating the following aspects:

- Collecting a database of tests of timber specimens under CPG, which could be used in future studies for validation and calibration purposes. The database can be downloaded as supplementary electronic material.
- Critical review of the current CPG capacity model, included in the draft of the next generation of Eurocodes.
- Comparison between eight probabilistic and deterministic capacity models to verify if the assumptions of the Eurocode model (especially those on the load spreading) have a solid foundation.
- Improvement and possible simplification of the Eurocode model, given the optimal fitting of the simplistic mechanical model and the probabilistic ones. This paper recognizes two candidate models for possible future code developments.

The paper has the following organization. Sec.3 presents the mechanical model and some literature background. Sec.4 shows the four studies used for the database compilation, further discussed in Sec.5, where a sensitivity analysis is carried out. Finally, Sec.6 compares several mechanical models by highlighting each formulation's possible pros and cons.

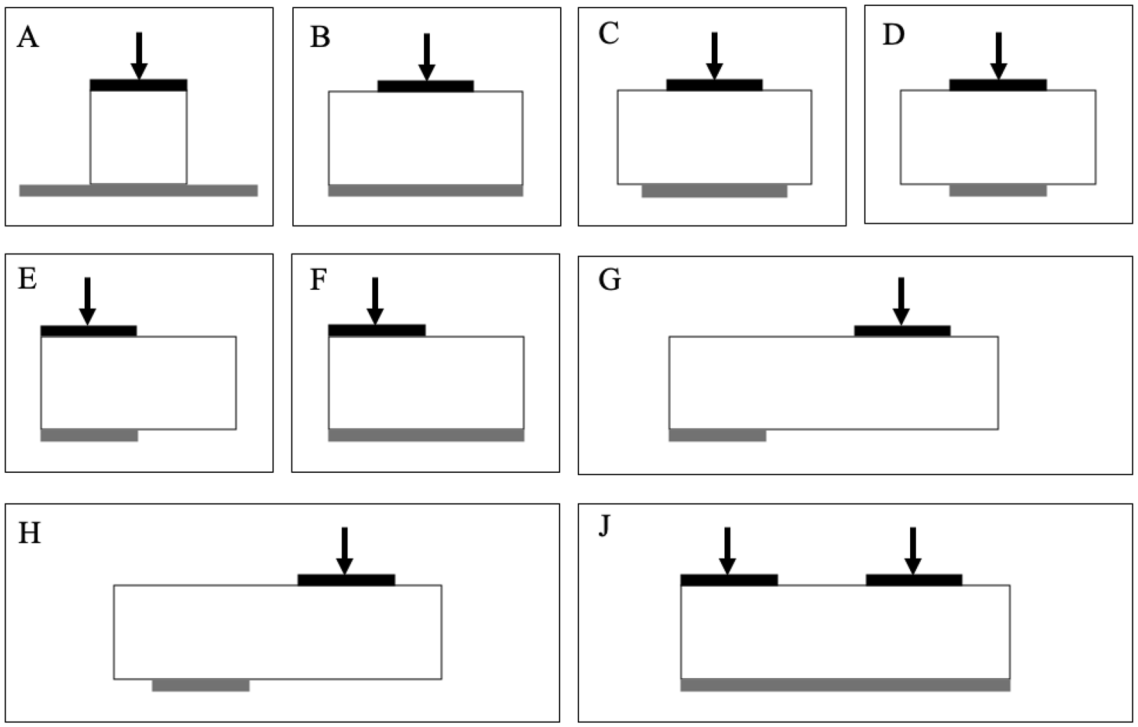

Fig. 4 Load cases definition according to Leijten (2016). A-E define symmetric loading configurations. F-J correspond to situations where the loading is eccentric to the reaction force.

3 Standard proposal and literature background

The design model in the current EN 1995-1-1 is presented as follows (EN1995 2010):

$$\sigma_{c,90,d} \leq k_{c,90} \cdot f_{c,90,d} \tag{1}$$

where $\sigma_{c,90,d}$ is the stress level given by the effective contact area. The factor $k_{c,90}$ accounts for the material behaviour and the deformation perpendicular to the grain. Generally, this factor is considered equal to 1.0. Still, for specific support conditions (when higher deformation perpendicular to grain can be considered acceptable), the CPG capacity can be increased (the different support conditions are further specified in Eurocode 5 (EN1995 2010)).

In the new standard proposal (prEN1995 2021), a factor k_p is introduced, which also accounts for the material behaviour and the deformation perpendicular to the grain. In the new standard proposal, a coefficient $k_{c,90}$ is introduced, but with a different physical meaning related to the effects of the load arrangement. To avoid confusion when discussing the different standard proposals, the factor $k_{c,90}$ of the current EN 1995-1-1 version is indicated as k_{pr} (to be distinguished from k_p, which in the new standard proposal prEN 1995 is proposed only for the un-reinforced configuration). The effective contact area, A_{ef}, accounts for the contribution of adjacent fibres. A 30mm increase in the contact length on both sides of the contact area is recommended. The effective length considers the load distribution of the CPG stress, where the stress distributes to the unloaded timber parts.

The synoptic table in Table 3 shown below resumes the proposed design models for un-reinforced and reinforced timber members under CPG. A detailed definition of the notation is given at the beginning of the paper (Fig. 5). Eq. 3 shows the design model of the current Eurocode 5 proposal for non-reinforced specimens (EN1995 2010).

The new standard draft (prEN1995 2021) enclosed a design equation (Eq. 5) for reinforced timber members under CPG. The bearing capacity can be primarily increased by reinforcing the member with fully threaded self-tapping screws. The screws can vary in diameter, head, and length. Threads along the whole length reduce the risk of pushing in due to the bond between the screws and timber. The design model represents an evolution of the one in Eq. 3 for non-reinforced members. Three failure modes may occur: failure due to the withdrawal of the screw, failure due to buckling of the screw, or failure of timber, as confirmed by the investigations by Bejtka and Blaß at the University of Karlsruhe (Bejtka and Blaß 2004).

Table 3 Synoptic table of the design models for un-reinforced and reinforced timber members under CPG

Design model of timber members under CPG
Characteristic strength of non-reinforced members under CPG (EN1995 2010)
$\sigma_{c,90,d} \le k_{pr} \cdot f_{c,90,d}$ (2)
Note k_{pr} is originally indicated as $k_{c,90}$ in EN 1995-1-1 as in the Eq. 1. The new term is here adopted to be coherent with the new proposal.
Characteristic strength of non-reinforced members under CPG (prEN1995 2021)
$\sigma_{c,90,d} \le k_p \cdot k_{c,90} \cdot f_{c,90,d} = B_1$ (3)
$k_{c,90} = \sqrt{\frac{l_{ef}}{l_c}} \le 4$ (4)
Characteristic strength of reinforced members under CPG (prEN1995 2021)
$F_{c,90,k} = \min \begin{cases} k_{pr} \cdot b_c \cdot l_{ef,1} \cdot f_{c,90,k} + n \cdot min\{F_{w,k}, F_{c,k}\} = A_{11} + n \cdot A_{12} = A_1, \\ b \cdot l_{ef,2} \cdot f_{c,90,k} = A_2 \end{cases}$, (5)
for intermediate support
$l_{ef,1} = l_c + \min\{30\text{mm}, l_c, l_s/2\} + \min\{30\text{mm}, l_c, l_s/2\}$
$l_{ef,2} = 2l_r + (n_0 - 1) \cdot a_1$ (6)
for end support
$l_{ef,1} = l_c + \min\{l_e, 30\text{mm}, l_c, l_s/2\} + \min\{30\text{mm}, l_c, l_s/2\}$
$l_{ef,2} = l_r + (n_0 - 1) \cdot a_1 + \min\{l_r, a_{3,c}\}$ (7)
Screw withdrawal resistance
$F_{w,k} = \pi \cdot d \cdot l_w \cdot f_{w,k}$, where $f_{w,k} = 8.2 \cdot k_w \cdot k_{mat} \cdot d^{-0.33} \cdot \left(\frac{\rho_k}{350}\right)^{k_\rho}$ (8)
Screw buckling resistance
$F_{c,k} = \frac{\gamma_R}{\gamma_{M1}} \cdot \kappa_c \cdot N_{pl,k}$, where $N_{pl,k} = \pi \cdot \frac{d_1^2}{4} \cdot f_{y,k}$ and $\frac{\gamma_R}{\gamma_{M1}} \approx 1.18\,(*)$ (9)
$(*)$ $\frac{\gamma_R}{\gamma_{M1}}$ can be assumed equal to one for estimating the mean value of the buckling resistance

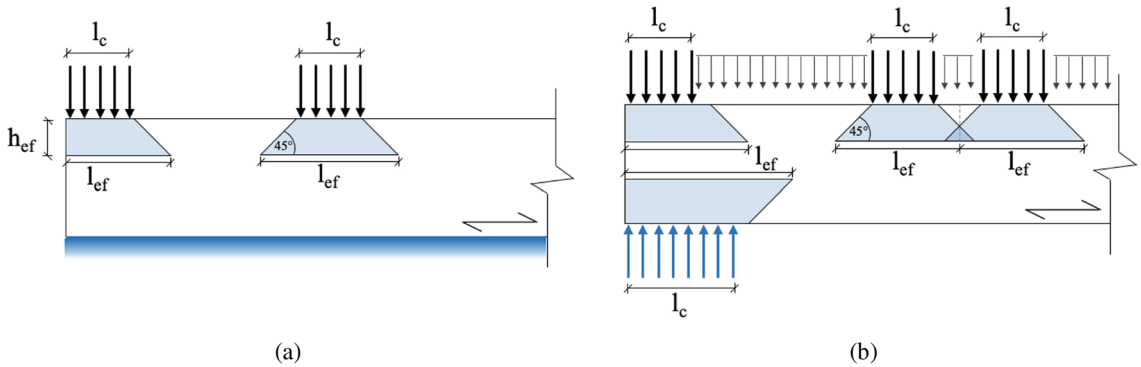

Fig. 5 CPG according to prEN1995-1-1, load dispersion for continuous (**a**) and discrete supports (**b**)

The first failure mode (Pushing-in of the screw) corresponds to the pushing-in capacity of the screws (withdrawal capacity $F_{w,k}$). Exceeding the bearing strength leads to penetration of the screws into the timber member. Numerous studies at the University of Karlsruhe have shown that the capacity to push in is equal to the withdrawal capacity. This failure mode occurs mainly using short screws (Bejtka 2005). The second failure mode corresponds to the buckling of the screws. This failure mode occurs mainly for long and slender screws. The third failure mode corresponds to timber failure at the screw tips. The feature of this failure mode is lateral expansion perpendicular to the grain, resulting in cracks at the screw tip.

Bejtka (2005) observed this failure mode with small loading areas and short screws. The maximum stress in the timber specimens by the screw tip depends on the effective dispersion length and width. The effective length depends on the size of the screw, the screw arrangement, and the design situation; see Fig. 7. The numerical investigations by Dietsch et al. (2019) confirmed the expression for the

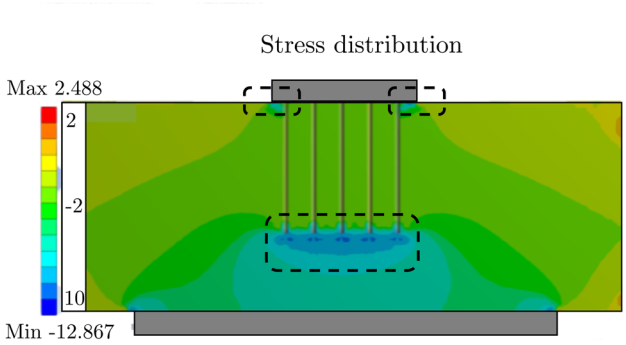

Fig. 6 Stress distribution of reinforced members, modified after Dietsch et al. (2019).

effective length, $l_{ef,2}$ in the third failure mode. The study investigated the effect of self-tapping screws as single-side reinforcement in timber (Dietsch et al. 2019). The study showed that the stresses varied extensively along the screw length, with a stress concentration by the tips of the screws, as shown in Fig. 6. However, the stress concentration is compensated for by stress redistribution due to the elastic-plastic behaviour of timber.

Figure 6 depicts the distribution of stresses in a horizontal plane along $l_{ef,2}$ with different screw groups (four, six, and ten). Figure 6 reveals that the stress increases by the screw tips. The study concludes with a recommendation for using screws with overlap to transmit the stress concentration efficiently. The first and second terms of Eq.3 correspond to the contributions by screws and timber, respectively. The withdrawal resistance, $F_{w,k}$, the compression resistance, $F_{c,k}$ and the number of screws, n, provide an estimate of the characteristic strength of the screws. Conversely, the effective contact length, $l_{ef,1}$, is increased by up to 30 mm, assuming the load will disperse at a 45° angle. The effective length at the screw tip is defined by $l_{ef,2}$, as depicted in Fig. 7.

PrEN 1995 is currently under development. Therefore, the reported equations represent an intermediate step toward a definite standard proposal. The synoptic table also provides the expressions for the withdrawal resistance, $F_{w,k}$, and compression resistance, $F_{c,k}$, of the screws. The authors adopted the following abbreviations to indicate the different contributions to the capacity. A_1 indicates the failure of the screw, where A_{11} and A_{12} separately express the contributions of timber and screws. A_2 represents the capacity related to the failure of the timber at the screw tip.

4 Database compilation

The database used to validate and calibrate capacity models for reinforced specimens under CPG with steel plates is based on the following experimental tests resumed in the appendix (Electronic Supplementary Material):

- Bejtka (2005);
- Nilsson (2002);
- Reichegger (2004);
- Tomasi et al. (2023).

Bejtka (2005) wrote Volume 2 of the Karlsruhe reports on CPG with reinforcement using fully threaded screws. He investigated the failure mechanisms and the influence of the screws based on multiple laboratory tests. The table in the appendix reports the geometry of specimens, screws, experimental capacity and the relative capacity increment compared to the non-reinforced case. The test result revealed that the capacity under CPG can increase up to 329 % using

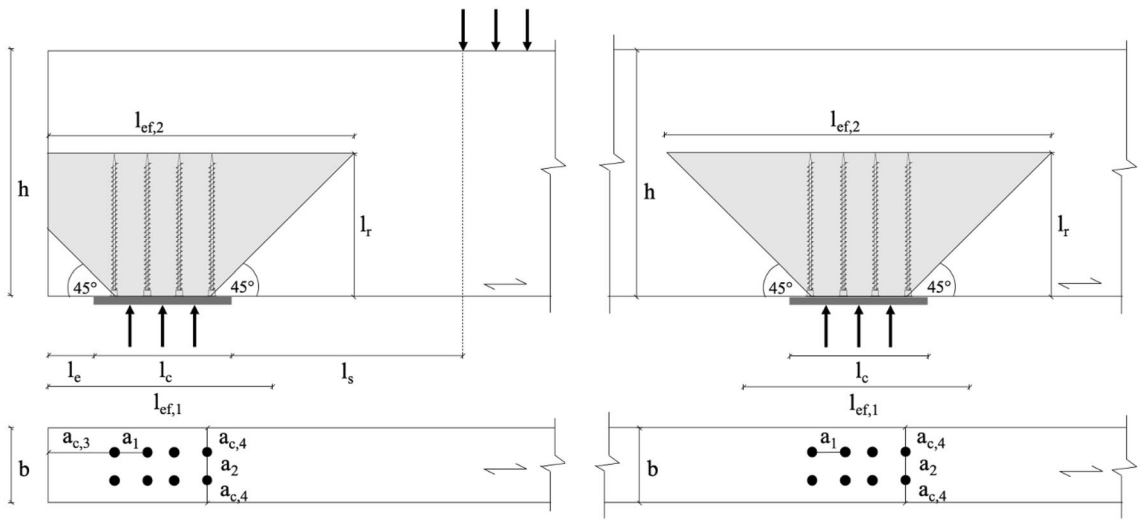

Fig. 7 Geometry of reinforced members subjected to CPG. The left and right figures indicate the beam's reinforcement by the edge and middle.

six screws. Furthermore, it is possible to improve the capacity further by using more screws. FE models in Ansys and experimental tests supported the development of a design model for reinforced members. The design model, known as the Model of Karlsruhe, is described in Eq. 10 (Bejtka 2005).

$$F_{c,90,Rk} = \min \begin{cases} k_{pr} \cdot b_c \cdot l_{ef} \cdot f_{c,90,k} + n \cdot R_{S,k} \\ b \cdot l_{ef,2} \cdot f_{c,90,k} \end{cases} \quad (10)$$

Where:

$$R_{S,k} = \min \begin{cases} R_{ax,k} = d \cdot l_s \cdot f_{w,k} \\ R_{c,k} = \kappa_c \cdot N_{pl,k} \end{cases} \quad (11)$$

The definition of the parameters is detailed in the initial list of symbols and notation. The model is analogous to the one in prEN 1995, except for minor discrepancies. Additionally, Bejtka (2005) validated the model using both the characteristic and mean strength perpendicular to the grain, $f_{c,90,k}$ = 3.0 N/mm^2 and $f_{c,90}$ = 5.0 N/mm^2 obtained from experimental tests. As expected, the predicted capacity is minor compared to the test results when using the characteristic value $f_{c,90,k}$ = 3.0 N/mm^2. A good correlation is observed with $f_{c,90}$ = 5.0 N/mm^2.

Nilsson (2002) wrote a master thesis on the influence of reinforcement on CPG based on experimental tests. Multiple glulam specimens with the dimensions 500 × 90 × 315 mm (length x width x height) were tested using the screws SFS WT-T 8.2 with different lengths. She considered two load cases: Torx and load case B with either one, four, six, or eight screws, where the Torx test corresponds to the test on a single screw. This research assesses the dependence between the number of screws and bearing strength. The group of screws is loaded through a steel plate with dimensions 90 × 150 × 10 mm or a timber plate with dimensions 90 x 150 x 16 mm. The failure modes depend on the load plate (Nilsson 2002), as illustrated in Fig. 8, affecting the magnitude and location of the lateral expansion. Nevertheless, the test specimen is not split to verify the failure mode of the screw. In this paper, the authors will use the sole experimental data corresponding to samples loaded by steel plates. The specimens loaded with timber plates are insufficient to develop a probabilistic capacity model.

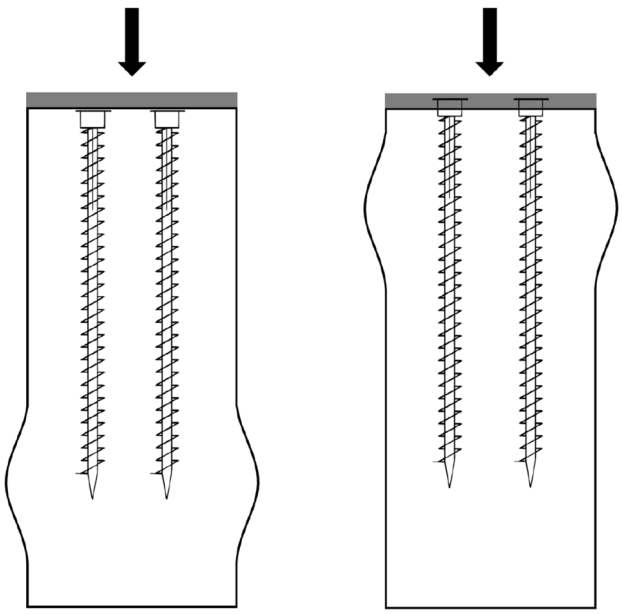

Fig. 8 Expansion of timber with steel plate (left) and timber plate (right), as observed by Nilsson (2002

Reichegger (2004) investigated the effect of self-tapping screws for members under CPG. The analysis is based on experimental tests and comparisons with the design model of Karlsruhe. He used spruce Glulam with strength class GL 24h according to EN 1194, with compressive strength $f_{c,90,k}$= 2.7 N/mm^2. The test specimens had dimensions 400 × 120 × 200 mm and 600 × 120 × 400 mm (length × width × height). The tests resemble load case B, where the load is applied by steel and timber plates with dimensions 80 × 120 and 120 × 120 mm, respectively. He used two types of screws: SFS WT-T and SPAX-S, where the mutual spacing is based on the ETA (European Technical Assessment) recommendation. The compressive capacity of the non-reinforced and reinforced test specimens is obtained following EN 1193, similar to the procedure described in EN 408. Furthermore, the study compares the test result to the Karlsruhe model. With a steel plate, the capacity increases up to 33 % and 167 %. Conversely, using a timber plate leads to an increment equal to 3 % and 124 % using WT-T 6.5 × 130 mm and SPAX-S 8 × 200 mm screws, respectively.

Tomasi et al. (2023) tested the accuracy of the design model for reinforced glulam members subjected to CPG, according to the new proposal of Eurocode 5 based on the Model of Karlsruhe in Eq. 10 (Bejtka 2005). Tomasi et al. (2023) present the experimental tests of multiple timber specimens with screw reinforcement under CPG by considering different geometry, load cases, and screw arrangement. Furthermore, the predicted capacity and failure modes are compared with the test results. The experimental results show that using threaded screws as reinforcement effectively increases the capacity of timber subjected to CPG. The experimental tests do not confirm the predictions regarding failure modes and capacities for all configurations.

4.1 Comparison with prEN 1995 model predictions

This section compares the design model of (prEN1995 2021) and the test results from past research. Nilsson (2002) and Reichegger (2004) transmitted the load by either a steel or timber plate, while Bejtka transferred the load with just a steel plate. The steel plate evenly distributes the force on the contact area and the screw heads. With a timber plate, the screws penetrate the timber plate, and the increase of capacity due to reinforcement may not occur (Bejtka 2005). As remarked above, since most of the tests are executed with steel plates, the investigation will neglect the CPG with timber plates for the load transfer.

The compiled database, to be downloaded as supplementary electronic material, compares the predicted capacity according to the two failure mechanisms (A_1 and A_2) and the estimated force at 1% deformation. The authors could note the experimental failure mode in most specimens, missing in the Karlsruhe report (Bejtka 2005) and Nilsson (2002). The k_{pr} assumed in the analyses is 1 for load case H, 1.5 for A, and 1 for B and C, following the definition in the initial list of notations. The additional parameters needed to calculate A_1 and A_2, especially the geometrical parameters of the screw and plate arrangements, are reported in the appendix (Electronic Supplementary Material).

There is a significant deviation between the test results obtained by Bejtka and the predicted load-carrying capacity. He investigated two load configurations, indirect (H) and direct (C) load arrangements. The spacing between the load and the support is less than two times the height for load case H. Thus, k_{pr} is considered equal to 1.0 for both cases. The observed failure mode is only reported in the preliminary tests. The failure mode for D_8a_6 is buckling, while the design model predicts the timber failure. Elsewhere, the failure modes agree with the predictions. In the tests by Bejtka, the highest capacity is achieved with six screws or four screws with a 10mm diameter. The significant variation in capacity depends on the different lengths and diameters of the screws. For most configurations, the A_1 is lower than the test results. The forces and predictions in load case H are generally lower than in case C. In H, the load dispersion is reduced considerably since the member is loaded near the edge.

In the tests by Nilsson (2002), the predicted failure modes follow A_2 for all configurations. Regrettably, Nilsson (2002) did not split the specimens to observe the failure mode. Additionally, the predicted capacity is consistently lower than the experimental values. Interestingly, the resistance for the test configuration with eight screws is lower than that with six. However, the recommended minimum spacing is not satisfied. This fact might increase the risk of splitting and result in a capacity reduction. The load situation is B, and A_2 is the estimated failure mode for all specimens. There is a significant gap between A_1 and A_2 due to the k_{pr} factor, assumed equal to 1.5 for A_1, whilst for A_2 k_{pr} is not considered.

In the study by Reichegger (2004), the specimens attained failure in the screws due to either buckling or withdrawal. The predicted and estimated failure modes are inconsistent since A_1 was consistently observed while A_2 was predicted. According to the design model, A_2 is the decisive capacity and is consistently lower than A_1. The A_1 capacity agrees with the experimental observations. The capacity of the screws is the minimum between buckling and withdrawal resistance. The predicted failure mode of WT-T 6.5 x 130 and WT-T 8.2 x 160 is withdrawal, while buckling occurred. The remaining screws fail due to buckling due to their significant slenderness.

The test data by Tomasi et al. (2023) is the more comprehensive, including three load cases, A, B and C. The experimental results show that using threaded screws as reinforcement effectively increases the capacity of timber subjected to CPG. However, the tests did not confirm the predictions on failure modes and capacities for all configurations. The A_2 failure mode never occurs despite the model predicting its occurrence in more than half of the tested specimens. Conversely, A_1 estimates conform with the test results for load case B. The predicted capacity is consistently lower in load case C. This might depend on the k_{pr} coefficient, assumed 1.5 and 1 for B and C, respectively. The overall predicted failure mode of A_1 is mainly confirmed, except for the shorter screws.

5 Sensitivity analysis

Before developing a probabilistic capacity model for reinforced members under CPG, a sensitivity analysis of the design model highlights the effect of variable dimensions on specimen capacity. This study and the previous experimental data will support a discussion on the limits of the current capacity model and the need for a more advanced proposal. In 2019, the CEN committee compared two models proposed in Eurocode 5 for non-reinforced members. The sensitivity study compared two approaches by Leijten and Blaß by varying the height and length of the specimen (Niebuhr and Sieder 2019). The current design model for CPG in prEN 1995 is a modified approach after Leijten. The author replicated the study in prEN 1995 for non-reinforced and reinforced members under load cases B and C, see Fig.4.

5.1 Non-reinforced specimens under CPG

Figure 9 displays load cases B and C used as reference configurations for the sensitivity analysis. The contact length is varied between 20 mm and 300 mm, while the height is

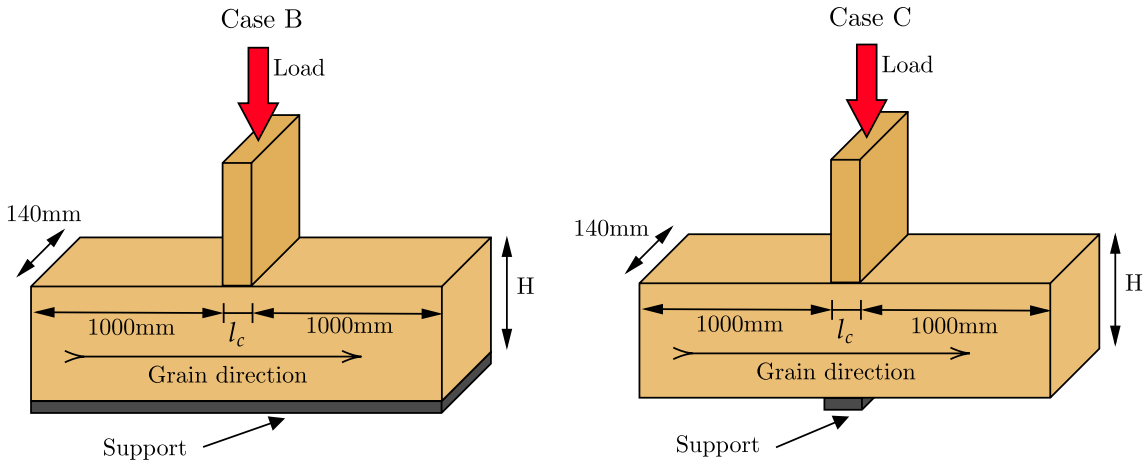

Fig. 9 Reference configuration of the non-reinforced members, with details on the geometry in load cases B and C. According to EN1995 (2010), k_{pr} is assumed to be equal to 1.5 for case B and 1 for case C.

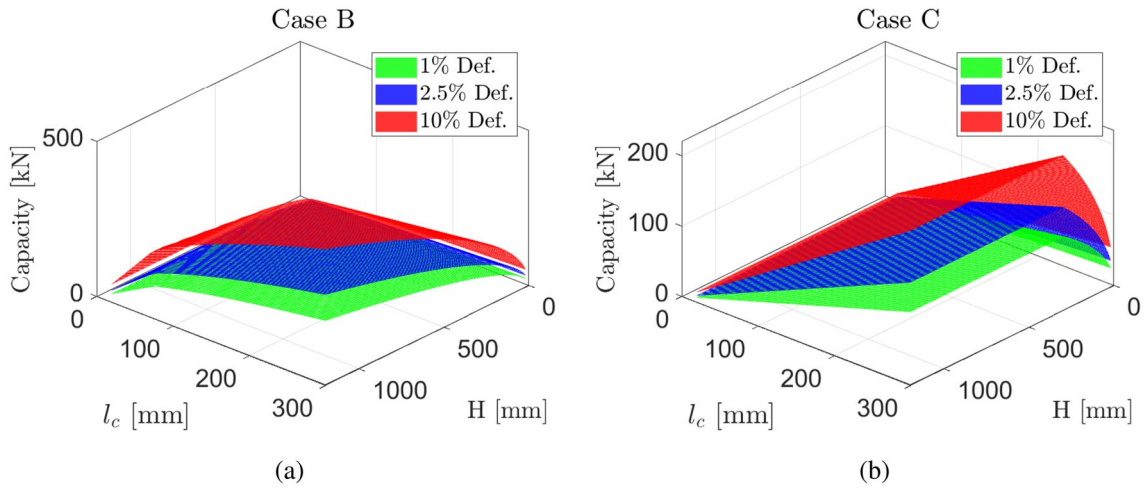

Fig. 10 Sensitivity analysis of the bearing capacity of the reference configuration in load cases B (a) and C (b). According to EN1995 (2010), k_{pr} is assumed to be equal to 1.5 for case B and 1 for case C.

between 20 mm and 1200 mm. The width and total length are set constant and equal to 140 mm and (2000 + l_c) mm, respectively. The characteristic properties of GL 30c are used in the calculations.

Figure 10 plots the bearing capacity corresponding to 1.0 %, 2.5 %, and 10 % deformation. The design model considers a non-linear increase in capacity with increasing deformation. The increase is significantly higher between 2.5 % and 10 % deformation, compared to 1.0 % and 2.5 % deformation. For 1.0 % deformation, the material behaviour factor, k_p, is equal to 1.0. For 2.5 % and 10 %, k_p is equal to 1.4 and 2.1, respectively (prEN1995 2021).

Figure 10 highlights the importance of the assumed limit deformation in the predicted resistance. The resistance is a highly conventional value, generally estimated at 1% deformation. The difference between the two cases is the load condition, which affects the load arrangement factor, $k_{c,90}$. In non-reinforced members, the load arrangement factor depends on the load dispersion due to the effective height and contact length. In discrete supports, the effective height is limited to 140 mm, while in continuous supports to 280 mm. Consequently, discrete supports have a lower $k_{c,90}$ factor. In discrete supports, the beam will exhibit additional deformation due to bending. Figure 10 shows a significant increase in capacity for load case B until the 280mm height is reached. After this point, the resistance is constant, despite the increase in height. After that, the capacity increases linearly with the contact length, although the increment rate is higher for case B than C. For case C, the member's height is reduced by using $0.4 \cdot H$ until the limit is reached.

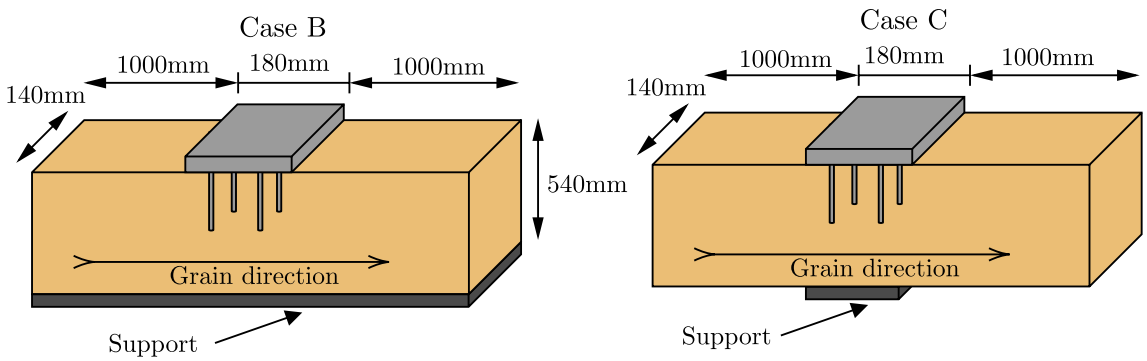

Fig. 11 Description of the reference case studies for reinforced members in load cases B and C. According to EN1995 (2010), k_{pr} is assumed to be equal to 1.5 for case B and 1 for case C.

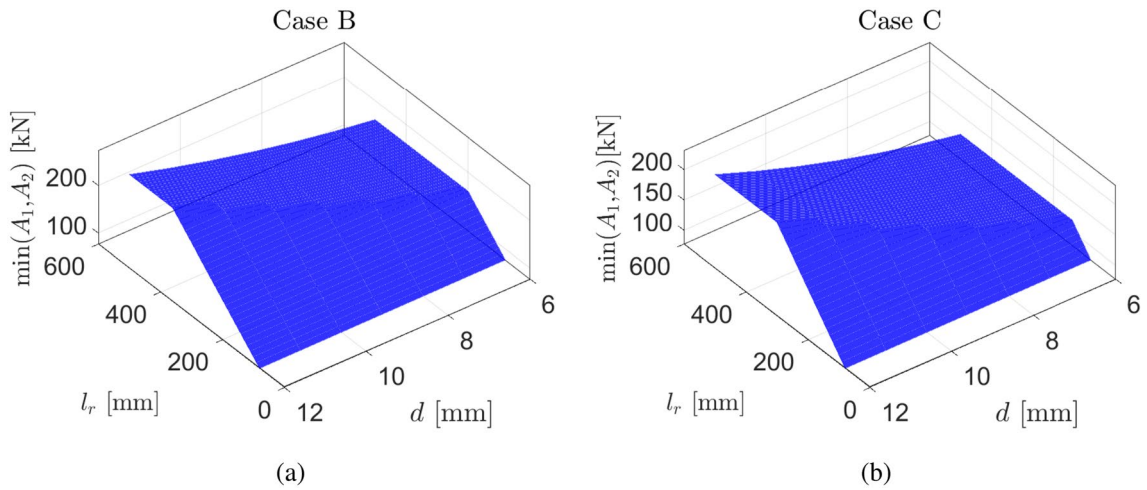

Fig. 12 Sensitivity analysis of the bearing capacity of the reinforced members for load cases B and C. According to EN1995 (2010), k_{pr} is assumed to be equal to 1.5 for case B and 1 for case C.

5.2 Reinforced specimens under CPG

Figure 11 shows the geometric details of the reference configurations in load cases B and C. In this subsection, the authors assess the sensitivity of the reinforced members to the screw length and diameter. The two variables have a decisive impact on capacity. In particular, the diameter and length affect A_1, while A_2 is affected by the screw length. The screw length varies between 80mm to 500mm. Following the standards' recommendations, the diameter varies between 6mm and 12mm. Other parameters, such as the contact length, member height, screw distance, and the number of screws, are considered constant. The characteristic values of timber correspond to GL 30c.

Figure 12 plots the resistance as the minimum between A_1 and A_2. Load case B leads to higher resistance than C. The capacity increases linearly with the screw length up to a specific value in both cases. Within this region, the screw diameter does not affect the capacity. The capacity increases with larger diameters when the screw length exceeds a specific length. Figure 13 separates the contributions A_1 and A_2.

A_2 does not change between the two load cases, increasing linearly with the length of the screw, while the screw diameter does not influence the capacity. When the screw length is small, the load-bearing capacity is driven by A_2. Conversely, when the screw length increases, the spreading length will also do. Therefore, beyond a specific screw length, A_1 becomes the predicted failure mode. The curves corresponding to A_1 are similar, but the capacities are different for the two load cases. Estimating A_1 is more convoluted since the capacity depends on both timber and screw contributions.

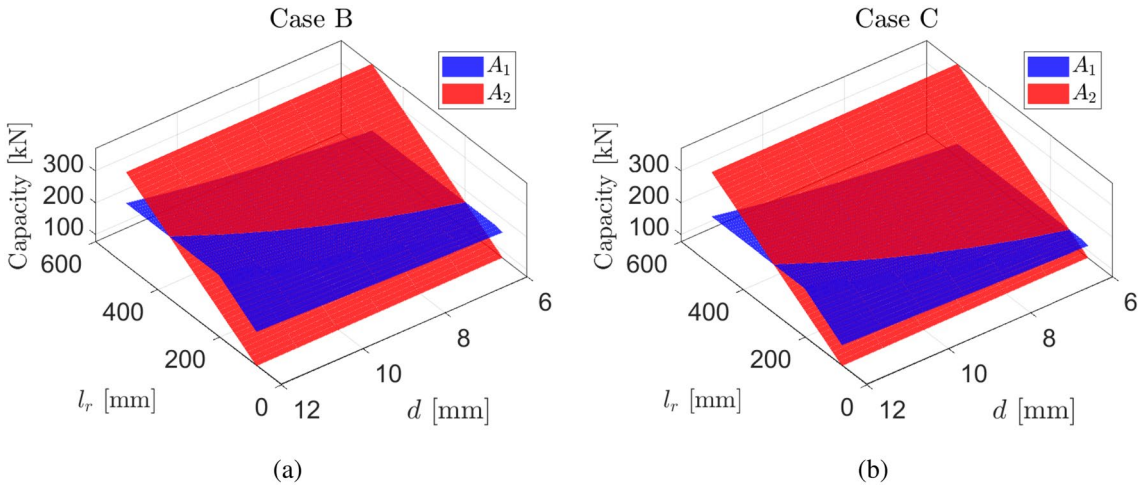

Fig. 13 Sensitivity analysis of the bearing capacity of the reinforced members for load cases B and C, where both A_1 and A_2 are plotted. According to EN1995 (2010), k_{pr} is assumed to be equal to 1.5 for case B and 1 for case C.

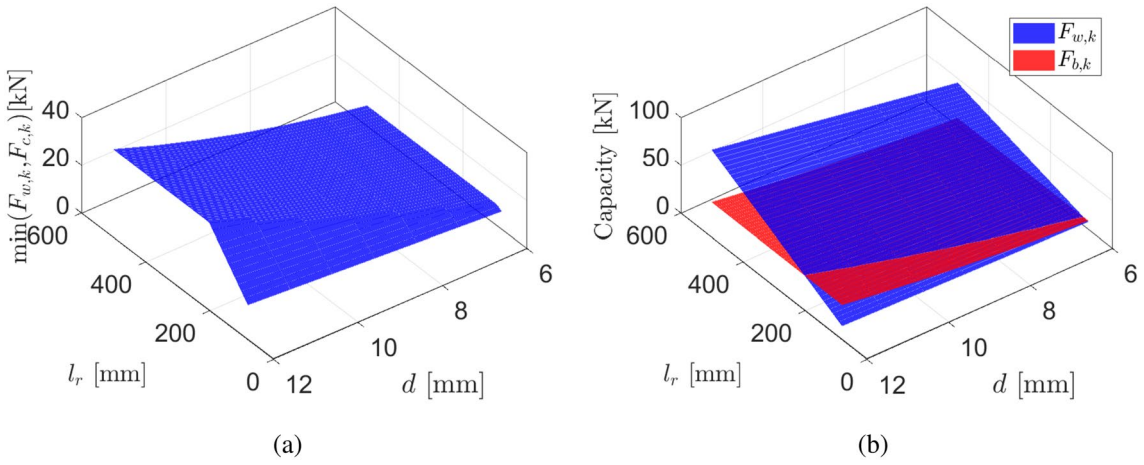

Fig. 14 Sensitivity analysis of the screws capacities, where the left figure displays $F_k = \min(F_{w,k}, F_{c,k})$, while the right one separately plots $F_{w,k}$ and $F_{c,k}$.

Figure 14 illustrates the capacity of one screw. The resistance of the screw is the minimum resistance between buckling and withdrawal. In Fig. 14a, F_k shows the same trend as A_1. As clarified above, the capacity stabilizes if the screw length reaches a specific level based on the screw diameter. Before this level is reached, the withdrawal capacity provides the minimum value. Subsequently, the buckling resistance gives the minimum. The buckling depends on the slenderness ratio of the screw, determined by the characteristic yield capacity of screws and the buckling load. The only parameter that varies in these formulas is the diameter. The buckling capacity is constant since it is not dependent on the screw length. In contrast, the withdrawal capacity depends on the screw length and diameter.

5.3 Justification for probabilistic models

The sensitivity analysis and the experimental results highlight the following possible limits of the current capacity model.

- The current capacity model estimates the capacity as the minimum between two failure modes. However, despite the model predicting the failure by the screw tips, the observed failure generally occurs by the contact area of the applied load. Additionally, the sensitivity analyses proved that the discrepancy between A_1 and A_2 reduces significantly if the minimum capacity is A_2. The inaccuracy of the A_2 failure mode might depend on the k_{pr} factor, affecting A_1, which increases the gap

between A_1 and A_2. The authors believe that the model can be simplified with a single capacity equation based solely on the first failure mode (A_1), properly corrected to include the effect of the screw length on the timber contribution.

- The model is deterministic. However, the availability of more experimental data might support the development of a probabilistic capacity model with a correction factor dependent on the geometric arrangement of the specimens.
- The model might be too complex, given its level of accuracy. The experimental data showed that the failure mode of the screws generally agrees with its prediction. Therefore, it might be helpful to correct the timber contribution with a single correction factor, dependent on adimensional geometrical parameters, given the significant uncertainty of this term.
- The differences between load cases can be expressed by synthetic geometric parameters rather than relying on the classification in Fig. 4. Avoiding such a classification and introducing a correction term, including the geometric feature characterizing the load configurations, might enhance the generality of the capacity model. Besides, the sensitivity analysis highlights a significant gap in the resistances for load cases B and C. However, the experimental predictions do not entirely confirm this gap. Therefore, a data-driven probabilistic capacity model might highlight the most significant parameters in the capacity model.

The following section will discuss a novel probabilistic capacity model for reinforced timber specimens under CPG obtained by calibrating a factor correcting the timber contribution characterized by higher uncertainty. The model will be simplified by replacing the effecting length with the contact area of the steel plate. Given the geometric limits by the standard, the correction factor will account for the uncertainty in the effective length and k_{pr} by calibrating a suite of explanatory variables dependent on the geometric arrangement of the specimen.

6 Comparison between capacity models

This section compares the performance of eight capacity models, resumed in the following synoptic Table 4.

To properly compare experimental data with model predictions, the mean values of the mechanical parameters replaced the characteristic ones. The first two models labelled $F^1_{c,90,m}$ and $F^2_{c,90,m}$, correspond to the first and the second failure mechanisms, known as A_1 and A_2. The authors separately compare each model prediction with the data to understand whether the proposed A_1 expression performs better when used without evaluating the minimum between A_1 and A_2 ($F^3_{c,90,m}$). The fourth model, $F^4_{c,90,m}$, is the simplistic capacity model. The timber contribution is obtained by multiplying the contact area by the strength of the timber perpendicular to the grain without any coefficient. The 5th

Table 4 Synoptic table of the design models for un-reinforced and reinforced timber members under CPG

Capacity models of timber members under CPG
1. Capacity model for the 1st failure mode according to the EC5 proposal
$F^1_{c,90,m} = A_1 = k_{pr} \cdot f_{c90,m} \cdot b_c \cdot l_{ef,1} + n \cdot \min\{F_{w,m}, F_{c,m}\}$ (12)
2. Capacity model for the 2nd failure mode according to the EC5 proposal
$F^2_{c,90,m} = A_2 = b \cdot l_{ef,2} \cdot f_{c90,m}$ (13)
3. Capacity model according to the EC5 proposal
$F^3_{c,90,m} = \mathrm{Min}(A_1, A_2)$ (14)
4. Simplistic model for the 1st failure mode
$F^4_{c,90,m} = A^*_1 = b_c \cdot l_c \cdot f_{c90,m} + n \cdot \min\{F_{w,m}, F_{c,m}\}$ (15)
5. Probabilistic model with adimensional explanatory functions and variance stabilizing transformation (P.M.1)
$F^5_{c,90,m} = \left[f_{c90,m} \cdot b_c \cdot l_c \cdot 10^{\gamma_1} + n \cdot \min(F_{w,m}, F_{c,m})\right]$ (16)
6. Probabilistic model with adimensional explanatory functions and variance stabilizing transformation (P.M.2)
$F^6_{c,90,m} = \left[f_{c90,m} \cdot b_c \cdot l_c \cdot \gamma_2 + n \cdot \min(F_{w,m}, F_{c,m})\right]$ (17)
7. Simplistic model for the 1st failure model with correction factor
$F^7_{c,90,m} = \gamma_3 \cdot b_c \cdot l_c f_{c90,m} + n \cdot \min\{F_{w,m}, F_{c,m}\}$ with $\gamma_3 = 2$ (18)
8. Simplistic model for the 1st failure model with correction factor derive from CPG formulation without reinforcement
$F^8_{c,90,m} = \gamma_4 \cdot b_c \cdot l_c f_{c90,m} + n \cdot \min\{F_{w,m}, F_{c,m}\}$ with $\gamma_4 = 1.4$ (19)
The variables with subscript $_m$ have replaced those with $_k$ to obtain the mean values.

and the 6th models, labelled $F^{5}_{c,90,m}$ and $F^{6}_{c,90,m}$, identify two probabilistic capacity models. The experimental data and existing capacity models prove that the higher uncertainty in the equation stands in the timber contribution. Several coefficients and arbitrary assumptions about the load diffusion affect this term, while the screw addend is generally considered as it is. Therefore, the authors calibrated a correction factor for the sole timber contribution as a function of a suite of explanatory variables. In the first probabilistic model (P.M.1), the experimental data were pre-processed with a variance stabilizing transformation. No variance stabilizing transformation is applied in the second one (P.M.2). The relevance of these models also depends on their generality. The multiplication factors, named γ_1 and γ_2, model an adimensional expression, the ratio between the expected and estimated timber contribution. Therefore, the authors selected adimensional geometric functions as candidate explanatory functions. A step-wise model reduction is then implemented to reduce the model, thus reaching a trade-off between complexity and accuracy. Lastly, the authors compare two deterministic models where the timber contribution is amplified by factors 2 and 1.4, respectively. The first factor is obtained from an ordinary least squares estimation, while the second is based on the formulation for CPG without reinforcement, where 1.4 is adopted.

This section might help the scholar and the practitioner understand the pros and cons of existing capacity models. This research's principal limitation is the modest number of test data. Approximately 60 samples might not be adequate for statistics. Despite the constraints, the authors propose probabilistic capacity models, which may be subjected to further calibration if more experimental data is added to the collected database. For this reason, the authors did not implement a Bayesian calibration, which should be more appropriate when having more data samples. The model calibration has been carried out with a maximum likelihood estimation. This section will first introduce the probabilistic capacity model and then compare the eight models.

6.1 Probabilistic capacity models

The simplistic mechanics-based model of reinforced timber under CPG can be written as follows:

$$C(\mathbf{x},\boldsymbol{\Theta}) = \underbrace{f_{c90,m}\cdot b_c\cdot l_c}_{\text{Timber}} + \underbrace{n\cdot\min\left(F_{w,m},F_{c,m}\right)}_{\text{Screws}} = A^{*}_{11} + A_{12} = A^{*}_{1} \tag{20}$$

where the contact area replaces the effective length and k_{pr} is assumed equal to 1. $C(\mathbf{x},\boldsymbol{\Theta})$ is the capacity, $\mathbf{x}$ are the measurable capacity variables, and $\boldsymbol{\Theta} = \{\boldsymbol{\theta},\sigma\}$ are unknown model parameters. Following Gardoni et al. (2002), the proposed form of the capacity can be written as follows:

$$T\left[\frac{F^{exp} - A_{12}}{A^{*}_{11}}\right] = \gamma(\mathbf{x},\boldsymbol{\theta}) + \sigma\varepsilon, \tag{21}$$

where $T(\cdot)$ is a variance stabilizing transformation, $\gamma(\mathbf{x},\boldsymbol{\theta})$ is a correction term based on mechanics rules and evidence derived from the experimental data, F^{exp} is the experimental resistance. The product $\sigma\varepsilon$ is the model error, with model standard deviation σ and normally distributed random variable ε. The model is based on three assumptions: additivity (i.e., the additivity of $\sigma\varepsilon$); homoskedasticity (i.e., the independence of σ from $\mathbf{x}$); normality (i.e., the normality of ε). Through a suitable choice of $T(\cdot)$, such assumptions can be approximately satisfied in the transformed space within the range of the data used to calibrate the model.

The correction term $\gamma(\mathbf{x},\boldsymbol{\theta})$ is selected as a linear combination of n dimensionless explanatory functions $h_i(\mathbf{x})$ and reads

$$\gamma(\mathbf{x},\boldsymbol{\theta}) = \boldsymbol{\theta}^{\mathrm{T}}\cdot\mathbf{h}(\mathbf{x}). \tag{22}$$

The set of explanatory functions $\mathbf{h}(\mathbf{x}) = \{h_1(\mathbf{x}),..,h_n(\mathbf{x})\}$ is constructed starting from physical variables not included in A^{*}_{1} that may be relevant for the described physical phenomenon, but also from those included in A^{*}_{1} and the effect of which should be recalibrated in light of the available experimental data. The following set of explanatory functions is used, also reported in Table 5.

- $\left\{\frac{a_{3,c}}{b_c}, \frac{a_{3,c}}{l_c}, \frac{l_e}{b_c}, \frac{l_e}{l_c}, \frac{l_e a_{3,c}}{l_c b_c}, \frac{a_1}{b_c}, \frac{a_1}{l_c}\right\}$: These functions express the relative distance between the screws and the steel plate from the specimen edges. Additionally, the last two measure the screw spacing compared to the extension of the steel plate.
- $\left\{\frac{b_c}{H}, \frac{l_c}{H}, \frac{b_c l_c}{HW}\right\}$: These functions describe the plate extension compared to the specimen height.
- $\left\{\frac{n_0}{n}\right\}$: This term identifies the percentage number of screws oriented parallel to the grain.

Table 5 Set of candidate explanatory functions

Explanatory functions			
h_{11}	a_{3c}/b_c	h_{17}	a_1/l_c
h_{12}	a_{3c}/l_c	h_{21}	b_c/H
h_{13}	l_e/b_c	h_{22}	l_c/H
h_{14}	l_e/l_c	h_{23}	$(b_c l_c)/(WH)$
h_{15}	$(l_e a_{rc})/(WH)$	h_3	n_0/n
h_{16}	a_1/b_c	h_4	l_r/H

- $\left\{\frac{l_c}{H}\right\}$: This term is the only one taking into account the screw geometry. It expresses the ratio between the threaded length of the screw and the specimen height.

The experimental data cannot be compared with the characteristic resistance $F_{c,90,k}$. Therefore, the mean values of the strength perpendicular to the grain and yielding strength of steel replaced the characteristic values. The mean value $f_{c90,m}$, in Eq.23, is obtained by assuming a coefficient of variation equal to 0.61, following Bejtka and Blaß (2004), who indirectly identified 5MPa as the mean value for the compression perpendicular to grain since it yields a higher correlation with the experimental parameters. Therefore a Coefficient of Variation (CoV) equal to 0.12 is estimated by assuming $f_{c90,m} = 3$ MPa and $f_{c90,k} = 2.5$ MPa following Leijten et al. (2010) and Bogensperger et al. (2011).

$$f_{c90,m} = \frac{f_{c90,k}}{(1 - 1.64 \cdot 0.12)} \tag{23}$$

The mean yielding strength of steel is obtained by assuming a CoV equal to 0.08, based on the experimental data by Bejtka and Blaß (2005).

$$f_{y,m} = \frac{f_{y,k}}{(1 - 1.64 \cdot 0.08)} \tag{24}$$

At this stage, the estimates of the mean strength are compared with the experimental values, as in Eq. 21. In the first step, all the parameters are used for calibration. To facilitate the use of the model and its possible implementation into technical standards, proposing a model with a limited number of explanatory functions should be advisable without significantly compromising accuracy. Nonetheless, reducing the number of terms usually leads to a higher value of σ. Stepwise deletion allows finding a compromise between parsimony and accuracy. There are several procedures to apply stepwise deletion, and they mainly differ in the deletion criteria, such as the stepwise deletion based on p-values (Stone 1996). The stepwise deletion process used in this paper starts with a model that includes all the candidate explanatory functions and, at each step, removes the explanatory function with the highest coefficient of variation (CoV) of the corresponding θ_i, as proposed in Gardoni et al. (2002). Once an explanatory function is removed, the model is re-calibrated, and the deletion process is repeated. The deletion process ends when either σ grows beyond an undesirable threshold

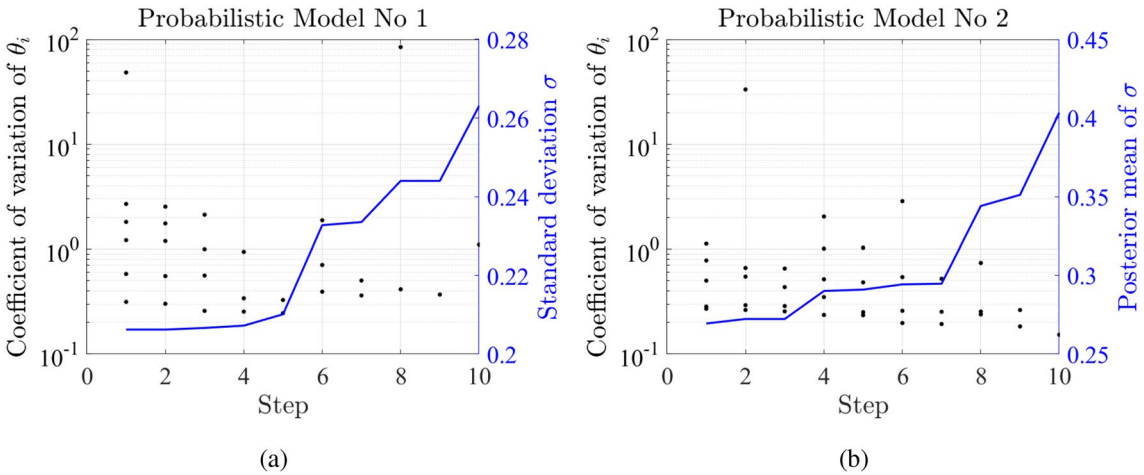

Fig. 15 Stepwise deletion process for the CPG model with (**a**) and without (**b**) variance stabilizing transformation.

Table 6 Statistics of $\boldsymbol{\Theta}$ of the probabilistic capacity model with variance stabilizing transformation

$\boldsymbol{\Theta}$	Mean	Stand. Dev.	Covariance coefficients						
			θ_0	θ_{12}	θ_{14}	θ_{16}	θ_{17}	θ_{22}	θ_3
θ_0	-0.246	0.255	0.065	0.002	-0.002	-0.057	-0.072	-0.011	-0.007
h_{12}	0.063	0.044	0.002	0.002	-0.001	-0.012	0.006	0.000	-0.002
h_{14}	0.015	0.028	-0.002	-0.001	0.001	0.006	-0.004	-0.001	0.001
h_{16}	-0.261	0.510	-0.057	-0.012	0.006	0.260	-0.122	-0.032	0.015
h_{17}	1.500	0.590	-0.072	0.006	-0.004	-0.122	0.348	0.041	-0.054
h_{22}	-0.055	0.151	-0.011	0.000	-0.001	-0.032	0.041	0.023	-0.001
h_3	-0.021	0.194	-0.007	-0.002	0.001	0.015	-0.054	-0.001	0.038

Table 7 Statistics of $\boldsymbol{\Theta}$ of the probabilistic capacity model without variance stabilizing transformation

$\boldsymbol{\Theta}$	Mean	Stand. Dev.	Covariance coefficients				
			θ_0	θ_{16}	θ_{21}	θ_3	θ_4
θ_0	2.248	0.538	0.104	-0.107	-0.012	-0.037	-0.040
θ_{16}	-2.640	0.940	-0.107	0.318	-0.010	-0.015	-0.040
θ_{21}	-1.401	0.496	-0.012	-0.010	0.089	0.009	-0.039
θ_3	0.544	0.403	-0.037	-0.015	0.009	0.058	0.007
θ_4	2.186	0.556	-0.040	-0.040	-0.039	0.007	0.111

or the increment of σ is too large compared to the reduction of the model complexity.

Figure 15 displays the CoV of the explanatory variables as a function of the number of steps for the two models with and without variance stabilizing transformation. The logarithm to base ten is used as variance stabilizing transformation in the first model, Fig. 15(b). In the same plot, the right y-axes show the standard deviation of the error as a function of the number of steps of the deletion process. The authors stopped at steps five and seven for the two models.

Figure15 highlights that after steps 5 and 7, there is a significant increment of the modelling error. Eqs.25, 26 report the final truncated expressions for the γ_1 and γ_2 correction terms in the two probabilistic models. Additionally, Tabs 6, 7 show the statistics of the coefficients of the explanatory functions of the two models, respectively.

$$\gamma_1 = \theta_0 + \theta_{12}\frac{a_{3,c}}{l_c} + \theta_{14}\frac{l_e}{l_c} + \theta_{16}\frac{a_1}{b_c} + \theta_{17}\frac{a_1}{l_c} + \theta_{22}\frac{l_c}{H} + \theta_3\frac{n_0}{n} \tag{25}$$

$$\gamma_2 = \theta_0 + \theta_{16}\frac{a_1}{b_c} + \theta_{21}\frac{b_c}{H} + \theta_3\frac{n_0}{n} + \theta_4\frac{l_r}{H} \tag{26}$$

The selected explanatory functions of the two models are not entirely the same. The γ_1 requires more terms, as discussed in the following paragraphs, to achieve a similar level of accuracy to the second model. The second model is more accurate than the first one. The lower values of the standard deviation of the first model, displayed in Fig. 15, depend on the different metrics, with and without the variance stabilizing transformation. In the first model, the authors are modelling the logarithm of the ratio. Table 8, discussed in the following paragraphs, compares the models' performances. It shows that the second model leads to a much better fitting despite γ_1 having seven terms and γ_2 just five. Interestingly, the second γ_2 does not include the terms expressing the distance of the load plate from the specimen edges. The relevant terms are just the density of the screws (a_1/b_c), the ratio between the plate width and the specimen height (b_c/H), the percentage number of screws oriented parallel to grain (n_0/n), and the ratio between the threaded length of the screw and the specimen height (l_r/H). The fact that the stepwise deletion neglects the distances from the edges is coherent with the good performance of the simplistic mechanical model, as discussed later.

It must be remarked that the dependence of the resistance on the explanatory functions is not straightforward to

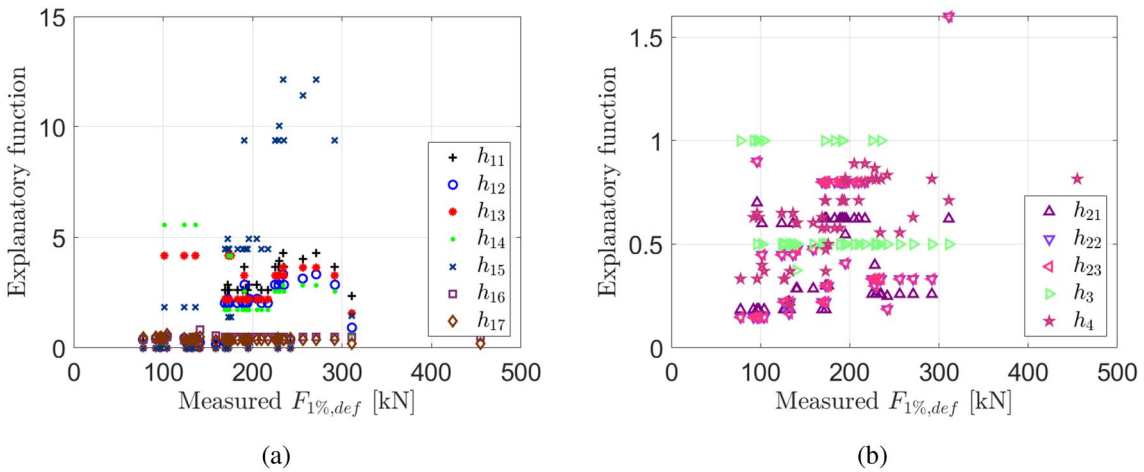

Fig. 16 Variation of the chosen explanatory functions with the measured resistance values. **a** refers to the explanatory functions in $\boldsymbol{h}_1$, while **b** to those in $\boldsymbol{h}_2$.

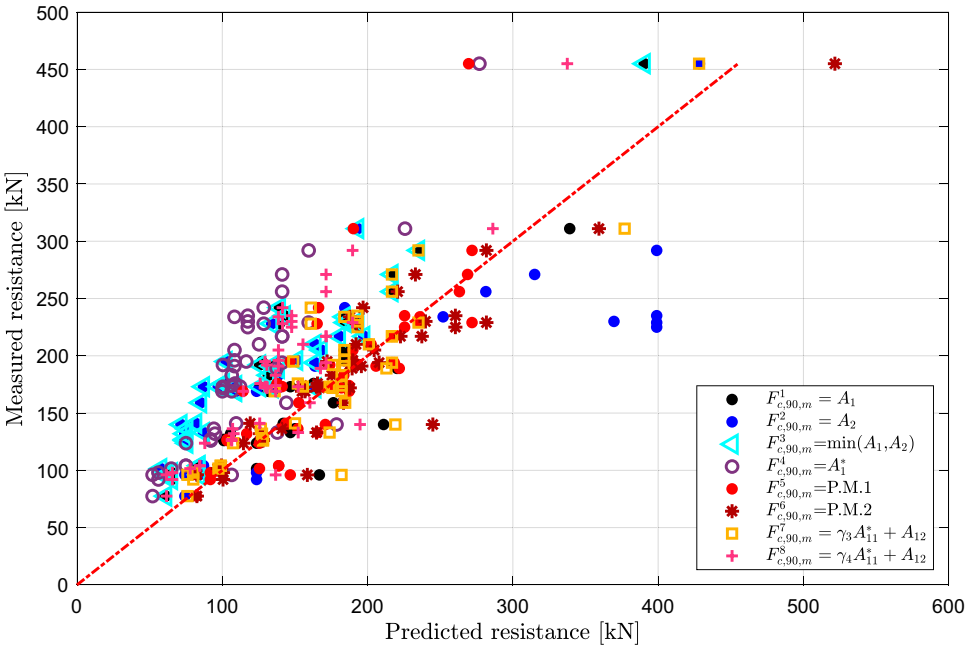

Fig. 17 Predicted vs measured force values for the eight considered capacity models

Table 8 Mean error, standard deviation (SD) and mean squared error (MSE), Maximum Absolute Error (MAE), Root Mean Squared Error (RMSE), Variance Accounted For (VAF) or the difference between measured and predicted force values. R^2 is the coefficient of determination of the fitting

Parameter	$F^1_{c,90,m}$	$F^2_{c,90,m}$	$F^3_{c,90,m}$	$F^4_{c,90,m}$	$F^5_{c,90,m}$	$F^6_{c,90,m}$	$F^7_{c,90,m}$	$F^8_{c,90,m}$
Mean	-21.52	-19.98	-52.20	-66.31	-7.71	2.70	-3.32	-42.83
SD	37.22	67.21	23.80	40.42	40.48	28.79	33.14	34.77
MSE	10546.59	30276.00	13876.84	31688.91	34386.98	11009.89	8395.49	13814.19
R^2	0.59	-0.08	0.27	-0.34	0.63	0.82	0.76	0.33
MAE	102.70	174.00	117.80	178.01	185.44	104.93	91.63	117.53
RMSE	89178.32	236366.53	160719.78	293843.71	81555.15	40136.55	53242.33	147933.97
VAF	1385.23	4516.86	566.44	1633.47	1638.44	828.71	1097.98	1208.98

understand from visual inspections; see Fig. 16. This fact entails the development of more complex capacity models, as carried out in this paper.

6.2 Comparison between capacity models

Fig. 17 and Table 8 compare the performances of the considered eight capacity models.

The performance of each model is discussed in a bullet point following a logic flow. Then, the comparison between models backs a conclusive discussion, highlighting the most suitable mechanical models and future research perspectives.

- Adopting A_2 as mechanical models leads to an extremely poor fitting. This fact is confirmed by the significantly high error and negative correlation coefficients occurring in rare circumstances in case of poor-quality regressions. This fact agrees with the experimental evidence, which showed that A_2 seldom occurs despite being predicted in multiple circumstances. Conversely, A_1 is in discrete agreement with the experimental data. The third capacity model, named $F^3_{c,90,m}$, is in the current EC5 proposal. Although the experimental data showed that it does not predict the failure modes, its performance is discrete. Therefore, using A_2 in some cases, rather than A_1, improves the model performance. The reason behind this might be the following: A_1 takes the load diffusion into account, which leads to a strength amplification not occurring in practice. Conversely, A_2 neglects this phenomenon, since $l_{ef,2}$ is generally lower than $l_{ef,1}$. Therefore, the discrete performance of the EC5 model does not depend on its mechanical background, contradicted by the experiments, but on error compensation. In some cases, A_2 better predicts failure mechanisms associated with A_1 because it neglects the model's assumed load diffusion.
- The fourth capacity model, $F^4_{c,90,m}$, is the simplistic model, where the timber contribution is obtained by multiplying the strength perpendicular to grain by the contact area of the steel plate. The performance is worse than the EC5 model, proving that the load diffusion occurs, despite not being entirely grasped by the EC5 model. The

performance of this model demonstrates that the load diffusion is not vertical, although lower than 45°, as proved by the first model. Nonetheless, the plate distances from the edges have a limited effect, and the stress bulb might have a steeper diffusion angle.

- The two probabilistic models have both satisfactory performance. However, the first one ($F^{5}_{c,90,m}$) with a variance stabilizing transformation has a modest performance compared to the number of terms involved. The relative error also increases compared to the simplistic mechanical model. Therefore, the first probabilistic model exhibits a good correlation, but its higher complexity does not yield a satisfactory accuracy gain. Conversely, the sixth model ($F^{6}_{c,90,m}$) has an outstanding performance. It is the best model among the eight for all error metrics with an $R^2 = 0.82$. An R^2 higher than 0.8 can be a good fitting for a mechanical model. Besides, the correction term for $F^{6}_{c,90,m}$ has just four addends, excluding the intercept. The four addends have a clear mechanical meaning and do not comprise the distances from the edges. This fact further confirms that the assumed diffusion model could be improved.
- The second model with the best performance is the $F^{7}_{c,90,m}$, where the correction term is assumed constant and equal to 2, as estimated from a least-squares optimization. This model can be recommended in standard applications due to its simplicity and high accuracy. Besides, this model is consistent with the one for CPG without reinforcement, which assumed an amplification factor equal to 1.4. $F^{7}_{c,90,m}$ and $F^{8}_{c,90,m}$ assume as coefficients for the timber contribution 1.2 and 1.4, respectively. Although the second coincides with the one for CPG without reinforcement, a 2 factor provides better performance in error metrics with $R^2 = 0.76$. The comparison between $F^{7}_{c,90,m}$ and $F^{8}_{c,90,m}$ proves that, if there are screws, the timber contribution amplifies and should be equal to 2.

In conclusion, the two models exhibiting the best performances are $F^{6}_{c,90,m}$ and $F^{7}_{c,90,m}$, in Eq.17 and Eq.18, respectively. The performance of the second probabilistic model is the best and highlights the most relevant variables to be included in a capacity model, neglecting those related to load diffusion. The deterministic model in $F^{7}_{c,90,m}$, obtained by assuming the correction factor constant and equal to 2, represents the optimal compromise between complexity and accuracy and might be the most suitable for standard implementation. Figure 17 plots the predicted vs the estimated resistance values for the eight capacity models. The figure establishes the above comments, proving the excellent fitting obtained with the 6th and 7th models.

Table 9 Maximum and minimum values of the explanatory functions of the model in Eq. 17

Explanatory functions			
Label	Definition	Min	Max
h_{16}	a_1/b_c	0.27	0.83
h_{21}	b_c/H	0.19	0.70
h_3	n_0/n	0.38	1.00
h_4	l_r/H	0.21	0.89

6.3 Discussion

The basis of the Eurocodes includes both mechanical principles and axiomatic truths. Therefore, in some instances, the formulations are not rigorous but strongly conventional. For example, that is the case of the assumptions behind the A_1 failure mechanism, where the load diffusion hypothesis results from conventional assumptions rather than mechanics. Still, a rigorous mechanical approach to this problem would be challenging to tackle with an analytical approach. Therefore, the main answer to this aspect should be found in the experimental data rather than in reasonable assumptions on the most likely structural response, i.e. a load diffusion at 45°. This assumption would be fair for isotropic materials but apodictic when applied to orthotropic materials with structural discontinuities (the screws, e.g.).

The probabilistic capacity model in Eq.17 demonstrates that a good regression can be obtained using a few adimensional parameters without considering those expressing the distances from the edges. However, the main limitations of the model are twofold: it is calibrated on a limited dataset, which might be inadequate for a good probabilistic formulation. Additionally, its validity can only be ensured within the limits of the adimensional parameters used for calibration. Therefore, Table 9 lists the selected explanatory functions with the maximum and minimum values from the chosen database.

However, given the uncertainty of this model, which could be further tested against more experimental data, hopefully coming from now on, the deterministic one in Eq. 18 could be a good compromise between complexity and accuracy. The model in Eq. 18 is analogous to the one for compression perpendicular to grain without reinforcement except for γ_3, equal to 2 rather than 1.4. Simplistic deterministic models might be preferable if they exhibit excellent accuracy. Besides, more experimental data would be needed for a more reliable probabilistic formulation.

7 Conclusion

This paper reviews existing capacity models for timber elements under compression perpendicular to the grain (CPG) with screw reinforcement. Eight mechanics-based

probabilistic and deterministic models have been compared against experimental values collected by the authors on test data from the past twenty years. The database consists of approximately 60 test data, which, despite being insufficient for an ideal probabilistic formulation, proved some weaknesses of existing formulations currently included in the draft of the next generation of Eurocodes. The main aspects that arise from the model's comparison and the analysis of the experimental data are:

- The formulations for predicting the assumed two failure mechanisms, one by the contact load (A_1) and the other by the screw tips (A_2), can be improved. The predicted failure mechanism (A_2) does not occur in more than half of the experimental data. Consequently, the A_1 predictive model performs better than $\min(A_1,A_2)$. Still, the model defined as $\min(A_1,A_2)$ possesses a discrete accuracy compared to A_1.
- The above observation might prove that the main shortcoming of the A_1 model stands in the assumed diffusion mechanism of the load. Contrary to the EC5 assumptions, the load diffusion is not at 45°, as confirmed by the good prediction of the mechanical model No 7 obtained by summing the screw and timber contribution amplified by a constant coefficient. The timber contribution is obtained by multiplying the timber strength by the contact load without any assumption about the stress spreading and the relative position of the loading plate to the specimen edges. The simplistic model yields an R^2=0.76 vs an R^2=0.59 for the model equal to A_1.
- The best fitting with the experimental data, with an R^2 =0.82, is obtained with a probabilistic model, where a factor corrects the timber contribution to resistance. The adimensional explanatory functions, selected by a stepwise deletion process, do not depend on the distances of the plate from the edges, proving that other parameters affect the resistance. Namely, the selected parameters are the density of the screws (a_1/b_c), the ratio between the plate width and the specimen height (b_c/H), the percentage number of screws oriented parallel to grain (n_0/n), and the ratio between the threaded length of the screw and the specimen height (l_r/H).
- The paper proposes a deterministic version of the probabilistic model, where the correction factor is assumed constant and equal to 2 after a least-squares optimization. This model represents a compromise between complexity and accuracy for future code developments.
- The experimental results do not confirm a significant difference between the analysed load cases classified in Fig. 4. Therefore, a unified coefficient k_{pr} is recommended for future standardisation.

This paper highlights the need for more experimental data for more reliable calibration of the probabilistic capacity model to extend its validity to a broader range of parameters.

Supplementary Information The online version contains supplementary material available at https://doi.org/10.1007/s00107-022-01918-z.

Acknowledgements The Authors kindly acknowledge the Master thesis students Eldbjørg Aaraas Hånde and Kari Ryen Thunberg for their contribution to the experimental work.

Funding Open access funding provided by Norwegian University of Life Sciences.

Data availability statement All data, models and code supporting this study's findings are available from the corresponding author upon reasonable request.

References

Aicher S (2011) Glulam beams with internally and externally reinforced holes - test, detailing and design. International Council for Research and Innovation in Building and Construction, Working Commission W18 - Timber Structures, Alghero, Italy. pp 1–13

Aicher S, Höfflin L (2002) Glulam beams with round holes-a comparison of different design approaches vs. test data, cib-w18/35-12-1. Proceedings of the International Council for Research and Innovation in Building and Construction, Working Commission W18-timber Structures

Aicher S, Höfflin L (2003) Design of rectangular holes in glulam beams. Otto-Graf-J. 14:211–229

Aicher S, Höfflin L (2009) Glulam beams with holes reinforced by steel bars. Intl. Council for Research and Innovation in Building and Construction, Working Commission 18-Timber Structures, Dübendorf, Switzerland

Aicher S, Höfflin L, Reinhardt HW (2007) Round holes in members made of glued laminated timber. part 2: Load capacity and design [Runde Durchbrüche in Biegeträgern aus Brettschichtholz, Teil 2: Tragfähigkeit und Bemessung]. Bautechnik 84(12):867–880. https://doi.org/10.1002/bate.200710074

Alinoori F, Moshiri F, Sharafi P, Samali B (2020) Reinforcement methods for compression perpendicular to grain in top/bottom plates of light timber frames. Constr Build Mater 231:116377

ASTM (1991) (the modernized metric system) Standard practice for the use of the international system of units (SI) (the modernized metric system). E 380-91a. Philadelphia, Pa.ASTM

Augustin M, Ruli A, Brandner R, Schickhofer G (2006) Behavior of glulam in compression perpendicular to grain in different strength grades and load configurations. In WCTE - 9th World Conference on Timber Engineering (pp. 829–836)

Basta C (2005) Characterizing perpendicular-to-grain compression in wood construction applications. Master thesis. Oregon State University. https://ir.library.oregonstate.edu/concern/graduate_thesis_or_dissertations/7p88ck24j

Bejtka I (2005) Verstärkung von Bauteilen aus Holz mit Vollgewindeschrauben (Reinforcement of wooden components with fully threaded screws). Doctoral dissertation, Universitätsverlag Karlsruhe. (in German language). https://doi.org/10.5445/KSP/1000003354

Bejtka I, Blaß HJ (2005) Self-tapping screws as reinforcements in connections with dowel-type fasteners, cib-w18/38-7-4. Proceedings of the International Council for Research and Innovation in Building and Construction, Working Commission W18-timber Structures, Meeting 38, Karlsruhe, Germany

Bejtka I, Blaß HJ (2004) Reinforcements perpendicular to the grain using self-tapping screws. Proceedings, 8th world conference on timber engineering. Lahti, Finland

Blass H, Ehlbeck J, Kreuzinger H, Steck G (2004) Erläuterungen zu DIN 1052: 2004–08: Entwurf. Inkl, Berechnung und Bemessung von Holzbauwerken (Explanations to DIN 1052: 2004-08), 2nd edition, DGfH, Bruderverlag, Munich/Karlsruhe

Bogensperger T, Augustin M, Schickhofer G (2011) 1. Properties of clt-panels exposed to compression perpendicular to their plane. At the Conference. International Council for Research and Innovation in Building and Construction, Working Commission W18-Timber Structures1–15

Bogensperger T, Augustin M, Schickhofer G (2011) 2. Properties of CLT-panels exposed to compression perpendicular to their plane. In Proceedings to International Council for Research and Innovation in Building and Construction, Working Commission W18 - Timber Structures, Alghero (Italy) (pp. 1–15)

Brandner R (2018) Cross laminated timber (clt) in compression perpendicular to plane: Testing, properties, design and recommendations for harmonizing design provisions for structural timber products. Eng Struct 171:944–960. https://doi.org/10.1016/j.engstruct.2018.02.076

Code (2005) Eurocode 2: design of concrete structures-part 1–1: general rules and rules for buildings. British Standard Institution, London

Conway M, Mehra S, Harte AM, O'Ceallaigh C (2021) Densified wood dowel reinforcement of timber perpendicular to the grain: a pilot study. J Struct Integ Maint. 63:177–186

Conway M, O'Ceallaigh C, Mehra S, Harte A (2020) Reinforcement of timber elements in compression perpendicular to the grain using compressed wood dowels. pp 319–324

Crocetti R, Gustafsson P, Ed D, Hasselqvist F (2012) Compression strength perpendicular to grain - full-scale testing of glulam beams with and without reinforcement. Proceedings of COST Action FP1004 Early Stage Researchers Conference. pp 51–62

De Santis Y, Fragiacomo M (2021) Timber-to-timber and steel-to-timber screw connections: Derivation of the slip modulus via beam on elastic foundation model. Eng Struct 244:112798

Dietsch P, Brandner R (2015) Self-tapping screws and threaded rods as reinforcement for structural timber elements-a state-of-the-art report. Constr Build Mater. https://doi.org/10.1016/j.conbuildmat.2015.04.028

Dietsch P, Gamper A, Merk M, Winter S (2015) Monitoring building climate and timber moisture gradient in large-span timber structures. J Civil Struct Health Monit. 52:153–165. https://doi.org/10.1007/s13349-014-0083-6

Dietsch P, Rodemeier S, Blaß H (2019) Transmission of perpendicular to grain forces using self-tapping screws. In: International network on timber engineering research INTER, meeting 6, Tacoma, USA

Ed D, Hasselqvist F (2011) Timber compression strength perpendicular to the grain - testing of glulam beams with and without reinforcement. Student Paper. Division of structural engineering; Civil Engineering (M.Sc.Eng.) Lund University

EN1995 (2010) EN 1995- 1-1.Eurocode 5: design of timber structures—part 1-1: general—common rules and rules for buildings

EN408 (2012) Timber structures —structural timber and glued laminated timber—determination of some physical and mechanical properties

ETA (2019) ETA-11/0030 European technical assessment. Screws for use in timber construction. ETA-Denmark, Nordhavn

Eurocode (2010) Eurocode 5: Design of timber structures - Part 1-1: General - Common rules and rules for buildings (2010) NS-EN 1995-1-1:2004+A1:2008+NA:2010

Forening, Norske Limtreprodusenters Norway, (2015) rette bjelker og søyler, limtreboka (vol. 2). Norske Limtreprodusenters Forening (Association of Norwegian Glued Manufacturers. The glue tree book (vol. 2 ed.). Norwegian Glued Tree Producers Association, John Grieg AS, Bergen

Frey-Wyssling A, Stüssi F (1948) Festigkeit und Vervormung von Nadelholz bei Druck quer zur Faser. (Strength and deformation of coniferous wood at pressure). Schweiz Z. Forstwes. 99(3):106–114

Gaber E (1940) Druckversuche quer zur Faser an Nadel- und Laubhölzern. (Compression tests across the grain on softwoods and hardwoods) Holz Roh- Werkst. 3(7–8):222–226. https://doi.org/10.1007/BF02717988

Gardoni P, Der Kiureghian A, Mosalam K (2002) Probabilistic capacity models and fragility estimates for rc columns based on experimental observations. ASCE J Eng Mech. 128(10):1024–1038

Gehri E (1997) Timber in compression perpendicular to the grain. IUFRO 5.02 timber engineering, Copenhagen, Denmark

Graf O (1921) Beobachtungen über den Einfluss der Größe der Belastungsfläche auf die Widerstandsfähigkeit von Bauholz gegen Druckbelastung quer zur Faser. (Observations on the influence of the size of the loading area on the resistance of timber to compressive loads perpendicular to the grain) (in German). Der Bauingenieur. 18:498–501

Harte A, Jockwer R, Stepinac M, Descamps T, Rajcic V Dietsch P (2015) Reinforcement of timber structures - the route to standardisation. Proceedings of the International Conference on Structural Health Assessment of Timber Structures, Shatis.'15: 78-89

Hassan K, Hussain T, Kamali A (2014) Compression perpendicular to grain in timber—bearing strength for a sill plate. Master Thesis Department of building technology, Linnéuniversitetet, Kalmar Växjö (Sweden)

Hübner U (2013) Mechanische Kenngrößen von Buchen-, Eschen- und Robinienholz für lastabtragende Bauteile (Mechanical characteristics of beech, ash and robinia wood for load-bearing components). Technical University publishing house. Monographic Series TU Graz. Timber Engineering & Technology. Series Editors G. Schickhofer and R. Brandner Institut für Holzbau und Holztechnologie

Hoffmeyer P, Damkilde L, Pedersen T (2000) Structural timber and glulam in compression perpendicular to grain. Holz Roh - Werkst. 58(1–2):73–80. https://doi.org/10.1007/s001070050390

Kevarinmäki A (1992) Strength of finnish softwoods in compression perpendicular to grain and reinforcment of support area with nail plates. Rakenteiden Mekani Ikka. 25:36–52

Kildashti K, Alinoori F, Moshiri F, Samali B (2021) Computational simulation of light timber framing connections strengthened with

self-tapping screws. J Build Eng. https://doi.org/10.1016/j.jobe.2021.103003
Kolb J (2008) Systems in timber engineering: loadbearing structures and component layers. Walter de Gruyter
Kollmann FF, Kuenzi EW, Stamm AJ (2012) Principles of wood science and technology: In wood based materials. Springer Science & Business Media, Berlin
Kreuzinger H (1999) Platten, Scheiben und Schalen-ein Berechnungsmodell für gängige Statikprogramme. (Plates, discs and shells-A calculation model for commonstatic programs) (In German).Bauen Mit Holz. 11:34–39
Kreuzinger H (2001) Verbundkonstruktionen. (Composite constructions) (In German). Holzbaukalender 2002:598–621
Kreuzinger H (2002) Holzbau. Handbuch für Bauingenieure, (Timber Construction. Civil Engineers Handbook) (In German). Springer, Berlin
Leijten A (2016) The bearing strength capacity perpendicular to grain of norway spruce-evaluation of three structural timber design models. Constr Build Mater. 105:528–535
Leijten A, Franke S, Quenneville P, Gupta R (2012) Bearing strength capacity of continuous supported timber beams: unified approach for test methods and structural design codes. J Struct Eng. 138(2):266–272
Leijten A, Larsen H, Van der Put T (2010) Structural design for compression strength perpendicular to the grain of timber beams. Constr Build Mater. 24(3):252–257
Madsen B, Hooley R, Hall C (1982) Design method for bearing stresses in wood. Can J Civil Eng. 9(2):338–349. https://doi.org/10.1139/l82-035
Madsen B, Leijten AJ, Gehri E, Mischler A, Jorissen A (2000) Behaviour of timber connections. Timber Engineering. University of British Columbia (UBC) https://doi.org/10.1139/l01-016
Maurer B, Maderebner R (2021) Cross laminated timber under concentrated compression loads-methods of reinforcement. Eng Struct. 245:112534
Mestek P (2011) Punktgestützte Flächentragwerke aus Brettsperrholz (BSP)-Schubbemessung unter Berücksichtigung von Schubverstärkungen [Cross laminated timber (clt) plane structures under concentrated loading from point supports-shear design including reinforcements]. Dissertation, Fakultät für Bauingenieur- und Vermessungswesen, Technische Universität München, Munich, Germany
Moerman B, Li M, Cao Y, Lim H (2021) Compressive behaviour of hardwood dowel reinforced clt loaded perpendicular-to-grain. Constr Build Mater. https://doi.org/10.1016/j.conbuildmat.2021.124137
Niebuhr P, Sieder M (2019) 01. Comparison of design models for timber in compression perpendicular to grain. CENCEN/TC 250/SC 5/PT 3 /N 26
Nilsson K (2002) Screw reinforcement as reinforcement in wood when loaded perpendicular to the grain direction: an experimental study (in Swedish). Master Thesis. Lund University, Sweden
O'Ceallaigh C, Harte A (2019) The elastic and ductile behaviour of clt wall-floor connections and the influence of fastener length. Eng Struct. 189:319–331. https://doi.org/10.1016/j.engstruct.2019.03.100
Orlando N, Taddia Y, Benvenuti E, Pizzo B, Alessandri C (2019) End-repair of timber beams with laterally-loaded glued-in rods: Experimental trials and failure prediction through modelling. Constr Build Mater 195:623–637
Pampanin S, Palermo A, Buchanan A (2013). Design guide Australia and New Zealand: Post-tensioned timber buildings—EXPAN design guides. Christchurch, New Zealand: Structural Timber Innovation Company
Persson K (2000) Micromechanical modelling of wood and fibre properties. Docotoral Thesis. Lund University, Department of Mechanics and Materials, Lund, Sweden
Porteous J, Kermani A (2013) Structural timber design to eurocode 5. Wiley, Hoboken
prEN1995 (2021) Eurocode 5: consolidated draft prEN 1995-1-1
Reichegger M (2004) Compressione ortogonale alle fibre negli elementi strutturali lignei secondo le nuove proposte di normative (Compression perpendicular to the grain in structural elements according to the new standard proposal) (in Italian). Master Thesis. Università Degli Studi Di Trento, Italy
Rothmund A (1944). Über die Wiederstandsfähigkeit des Holzes gegen Druck quer zur Faser (About the resistance of wood to pressure across the grain) (in German), Dissertation Technische Hochschule Stuttgart, Germany
Serrano E, Enquist B (2010). Compression strength perpendicular to grain in cross-laminated timber (clt). 1: 441-448
Stone CJ (1996) A course in probability and statistics (19). Duxbury Press, Belmont
Suenson E (1938) Zulässiger Druck auf Querholz. (Allowable compressive strength perpendicular to grain) (in German). Holz Roh-Werkst 1(6):213–216
Swedish Wood Stockholm, Sweden, (2016). Structural properties of sawn timber and engineered wood products, design of timber structures (vol. 1, 2nd ed. 1). Swedish Forest Industries Federation
Thelandersson S, Mårtensson A (1997) Design principles for timber in compression perpendicular to grain. Cib-w18, meeting 30, Vancouver
Tomasi R, Aloisio A, Hånde EA, Thunberg KR, Ussher E (2023) Experimental investigation on screw reinforcement of timber members under compression perpendicular to the grain. Eng Struct. 275:115163
Tomasi R, Crosatti A, Piazza M (2010) Theoretical and experimental analysis of timber-to-timber joints connected with inclined screws. Constr Build Mater. 24(9):1560–1571. https://doi.org/10.1016/j.conbuildmat.2010.03.007
van der Put T (2012) Restoration of exact design for partial compression perpendicular to the grain. Wood Mater Sci Eng. 7(4):225–236. https://doi.org/10.1080/17480272.2012.681703